Laboratories of General Pathology and Immunology "GiovannaTosi"

Department of Medicine and Surgery, School of Medicine

University of Insubria, Varese, Italy

Cytoplasmic Localization of HTLV-1 HBZ Oncoprotein: a Biomarker of HTLV-1-Associated Myelopathy/Tropical Spastic Paraparesis (HAM/TSP)

Marco Baratella

Ph.D Program "Experimental and Translational Medicine"

XXX Cycle

Project coordinator: Prof. Roberto S. Accolla

Project supervisor: Dr. Greta Forlani

Accademic year 2017/2018

ABSTRACT

Human T cell lymphotropic virus type 1 (HTLV-1) is the etiological agent of a severe form of T cell neoplasia called Adult T cell Leukaemia (ATL) and of a neurologic disorder designated *HTLV-1-associated myelopathy/tropical spastic paraparesis (HAM/TSP)*. The HBZ oncoprotein encoded by the minus strand of the HTLV-1 is thought to play an important role in both diseases.

The recent isolation in our laboratory of the first described monoclonal antibody against HBZ protein has now permitted to investigate in detail the cellular and biochemical features of endogenous HBZ. In this direction our laboratory has recently established that HBZ is a nuclear protein in cells of ATL patients. My thesis was predominantly focussed in expanding the analysis particularly in HAM/TSP patients, to assess similarities and/or diversities of HBZ subcellular distribution with respect to ATL patients and asymptomatic HTLV-1 carriers.

Expression and localization of HBZ in peripheral blood mononuclear cells (PBMC) of ATL, HAM/TSP patients and in HTLV-1 asymptomatic carriers (AC) was analyzed by immunohistochemistry and confocal microscopy using the anti-HBZ 4D4-F3 mAb. Analysis of patients with HAM/TSP unequivocally showed that HBZ-positive cells presented an exclusive, never reported, cytoplasmic localization of the viral oncogenic protein. Interestingly, experiment with leptomycin B indicated that HBZ could not shuttle between cytoplasm and nucleus. This strict HBZ cytoplasmic localization was at variance with the distribution of the other HTLV-1 oncogenic protein, Tax-1, that could localize both in the cytoplasm and the nucleus, and could be sequestered totally in the nucleus after leptomycin B treatment of the cells. Additional extensive analysis of cells from ATL patients and asymptomatic recipients confirmed, instead, a nuclear localization of HBZ.

I further supported this finding by studying HBZ and Tax-1 in the CIB cell line, a CD4+ IL-2-dependent T cell line derived from an HAM/TSP patient. The vast majority of CIB cells express significant amounts of HBZ exclusively in the cytoplasm, mostly in a speckle-like fashion. Tax-1 instead was expressed in 30% of the cells, either as a

diffuse reticulum or distributed in a speckled-like fashion mainly in the cytoplasm. Interestingly, in cells co-expressing cytoplasmic HBZ and Tax-1, the two proteins did not co-localize, suggesting that they do not interact *in vivo*.

Our results establish for the first time a distinctive and diverse pattern of sub-cellular localization of endogenous HBZ protein. Furthermore, and of potential importance in the pathogenesis of HTLV-1-associated diseases, our data suggest that the endogenous localization of HBZ protein in different cellular compartments may correlate with the different forms of the HTLV-1-mediated diseases.

1 INTRODUCTION

1.1 HTLV-1 infection and diseases

The human T-cell lymphotropic virus type 1 (HTLV-1) is the first described human retrovirus and belongs to the deltaviridae family, subfamily oncovirus type C (Poiesz et al., 1980). It is estimated that HTLV-1 has infected 10-20 million people world wide (Gessain and Cassar, 2012).

HTLV-1 infects primarily CD4+ T cells although other cell types such as CD8+ T cells, dendritic cells and B cells can also be infected, although more rarely.

As stated above, HTLV-1 was the first discovered human retrovirus associated with diseases (Poiesz et al., 1980). Indeed the virus is the etiological agent of a severe, still untreatable, form of adult T cell leukemia/lymphoma (ATL) as well as inflammatory syndromes (HTLV-1-associated myelopathy/tropical spastic paraparesis and uveitis among others). Finally, HTLV-1 is found associated also to opportunistic infections (including Strongyloides stercoralis hyperinfection and others).

1.1.1 Adult T-Cell Leukemia/Lymphoma

ATL is an aggressive lymphoproliferative malignancy of peripheral T cells, with short survival in its acute form and an incidence of less than 5% in HTLV-1-infected people. It was initially described in Japan and later in the Caribbean region and South America. In Europe and the United States, ATL was diagnosed in immigrants from regions of endemicity (Goncalves et al., 2010).

ATL is a heterogeneous, yet very aggressive, malignant disease clinically divided into four subtypes: acute, chronic, smoldering type and lymphoma type. Typical ATL cells have convoluted nuclei with homogeneous and condensed chromatin, small or absent nucleoli, and agranular and basophilic cytoplasm. The characteristic shape of the nucleus of ATL cells let to the designation of these cells as “flower cells”.

The rate of survival varies depending on the subtype: 4 to 6 months for the acute type, 9 to 10 months for the lymphoma type, 17 to 24 months for the chronic type, and 34 months to more than 5 years for the smoldering type.

1.1.2 HTLV-1-Associated Myelopathy/Tropical Spastic Paraparesis

HAM/TSP is a chronic meningomyelitis of the gray and white matter in the spinal cord, with perivascular demyelination and axonal degeneration (Cooper et al., 2009) with an incidence of less than 3% in HTLV-1-infected people. Patients will develop a slowly progressive spastic paraparesis, without remissions, with high impairment of gait, autonomic dysfunction of bladder and bowel, and profound repercussions on their abilities and quality of life. Women are affected more frequently than men, and the disease onset occurs in adulthood.

1.1.3 HTLV-1-Associated Uveitis

Ophthalmological disturbances related to HTLV-1 infection include vasculitis, exudation or degeneration of the peripheral retina, and keratoconjunctivitis sicca, as well as a typical form of uveitis (HTLV-1-associated uveitis or HAU) (Pinheiro et al., 2006)

Middle-aged HTLV-1-infected adults of both genders are the target population. HAU is characterized by a granulomatous or nongranulomatous reaction accompanied by vitreous opacities and retinal vasculitis with rare exudative retinochoroidal alterations in one or both eyes. It can occur as the only HTLV-1 manifestation or can be associated with HAM/TSP. Uveitis usually occurs as an isolated ophthalmological alteration.

Although the factors that cause the different manifestations of HTLV-1 infection are not fully understood, previous population studies suggest that both viral and host genetic factors influence the outcome of infection

1.2 The HTLV-1 Virus

HTLV-1 is an enveloped virus that is approximately 100 nm in diameter (Figure 1)

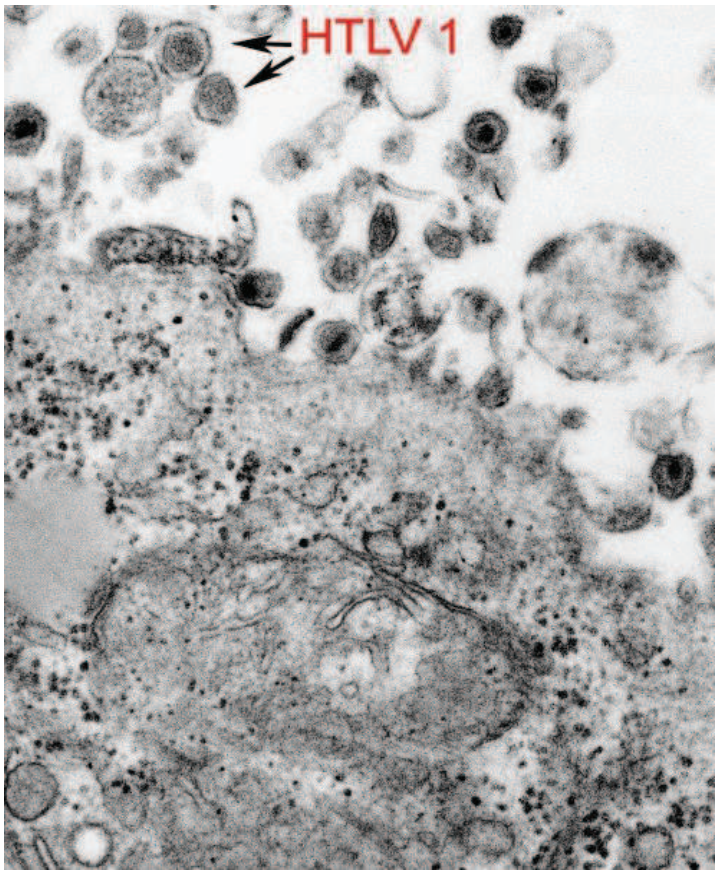

Figure 1. Electron Micrograph of HTLV-1. Arrows indicate the HTLV-1 virions. Image Adapted from Centers for Disease Control and Prevention, USA.

The inner membrane of the virion envelope is lined by the viral matrix protein (MA) (Figure 2). This structure encloses the viral capsid (CA), which carries two identical strands of the genomic RNA as well as functional protease (Pro), integrase (IN), and reverse transcriptase (RT) enzymes. A newly synthesized viral particle attaches to the target cell receptor through the viral envelope (Env) and enters via fusion, which is

followed by the uncoating of the capsid and the release of its contents into the cell cytoplasm. The viral RNA is reverse transcribed into double stranded DNA by the RT. This double stranded DNA is then transported to the nucleus and eventually integrated into the host chromosome forming the provirus. The provirus contains the promoter and enhancer elements for transcription initiation in the long terminal repeats (LTR); the polyadenylation signal for plus strand transcription is located in the 3′LTR (Kannian and Green, 2010)

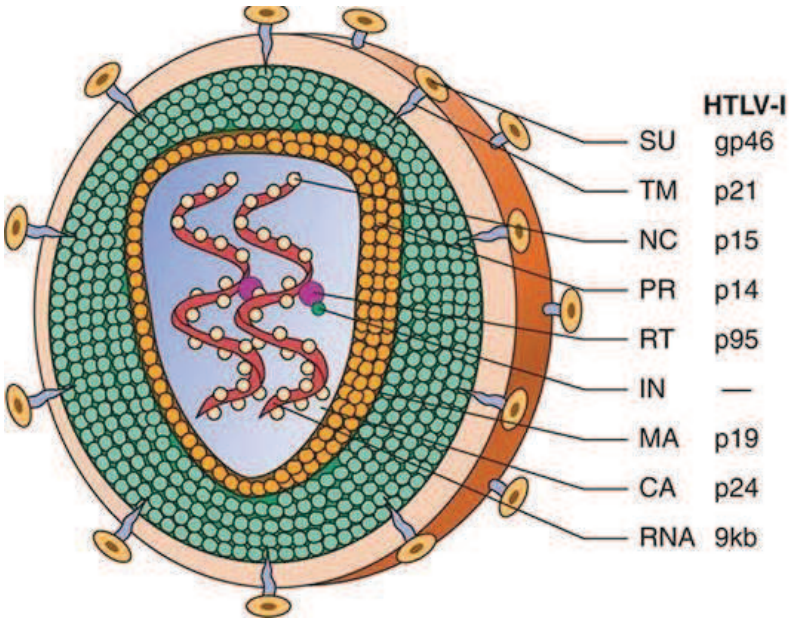

Figure 2. Schematic structure of HTLV-1. The surface glycoprotein (SU) is responsible for binding to receptors of host cells. The transmembrane protein (TM) anchors SU to the virus. NC is a nucleic acid–binding protein found in association with the viral RNA. A protease (PR) cleaves the polyproteins encoded by the *gag, pol*, and *env* genes into their functional components. RT is reverse transcriptase, The matrix protein (MA) is a Gag protein closely associated with the lipid of the envelope. The capsid protein (CA) forms the major internal structure of the virus, the core shell.

There are four known strains of HTLV including HTLV type 1 (HTLV-1), HTLV-2, HTLV-3 and HTLV-4. HTLV-1 and HTLV-2 were discovered in the 1980s (Poiez et al., 1980). HTLV-3 and HTLV-4 were only recently described (Mahieux and Gessain, 2009) (Nicolas et al., 2015). So far, the only strain that is clearly associated with human diseases is HTLV-1.

The most important routes of HTLV-1 transmission are breastfeeding, sexual intercourse, and blood contact, including the transfusion of infected cellular products or sharing of needles and syringes (Proietti et al., 2005)

1.3 HTLV-1 Genome

The genome organization of HTLV-1 is similar to all common retroviruses; in fact, HTLV-1 has *gag, pro, pol* and *env* genes that respectively encodes for structural protein of the virion (gag), the viral protease (pro) the reverse transcriptase enzyme (pol) and the virion envelope glycoprotein (env) (Figure 3).

In addition to essential retroviral components, HTLV-1 provirus has a unique region between *env* and the 3′LTR; and this region is named *pX* (Franchini et al., 2003). The *pX* region encodes viral regulatory and accessory proteins Tax, Rex, p8, p12, p13, p30, p21, and HTLV-1 bZIP factor (HBZ) which are implicated in viral infectivity and the proliferation of infected cells (Gaudray et al., 2002; Mota-Miranda et al., 2013; Satou et al., 2006). Tax is recognized as a potent oncoprotein, since it immortalizes human primary T cells by itself, and Tax transgenic mice form tumors (Tanaka et al., 1990). Nevertheless, *tax* transcripts are detected in only ~40% of ATL cases (Takeda et al., 2004). Recently, the viral factor, HBZ, has been shown to have an oncogenic effect in vivo (Satou et al., 2011). Expression of HBZ is conserved in all ATL cells, strongly suggesting that it contributes to leukemogenesis (Yasunaga and Matsuoka, 2011).

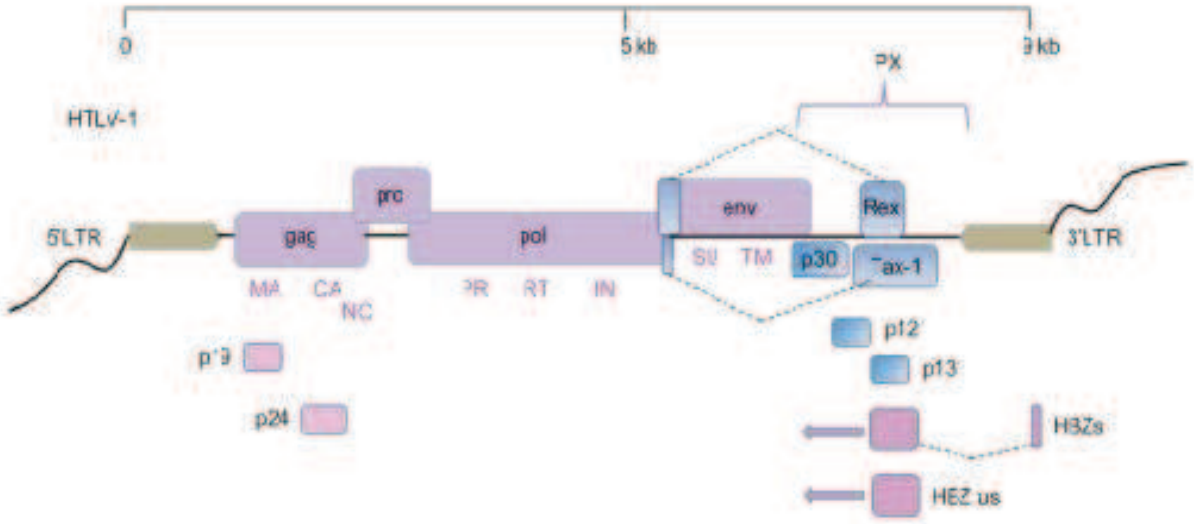

Figure 3. Schematic representation of HTLV-1 genome. p19 and p24 are the major core proteins of HTLV. Gray: LTR, Long Terminal Repeat; Coding regions for all major proteins: gag, group-specific antigen; pro, protease; pol, polymerase; env, envelope; rex, regulator of expression; tax, transactivator; HBZ, HTLV basic leucine zipper. The pink letters indicate the positions of the major proteins encoded by the corresponding genes, including the MA (matrix), CA (capsid), NC (nucleocapsid) proteins of gag, the PR (protease), RT (reverse transcriptase), IN (integrase) enzymes of pol and the SU (surface) and TM (transmembrane) proteins of env. (Zhang et al., 2017)

1.4 The HTLV-1 bZIP Protein (HBZ)

HBZ protein contains a bZIP domain in addition to an activation (N-terminus) and a central domain (Figure 4) (Gaudray et al., 2002).

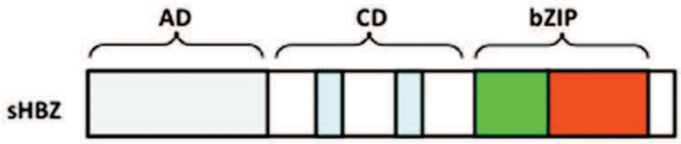

Domain	Function
AD	Bind with 26S proteasome Interact with CBP/p300 Activate TGF-β signaling
CD	Induce nuclear localization
bZIP	Interact and inhibit c-Jun, JunB, CREB, CREB2 Inhibit 5'LTR activation
AD+bZIP	Bind with p65, inhibit classical NF-kB pathway Ativate JunD Enhance hTERT promoter activity

Figure 4. Schematic representation of HBZ domains. HBZ has three domains: activation domain (AD), central domain (CD), and basic ZIP domain (bZIP). Functions of each domain are listed. (Zhao and Matsuoka, 2012)

There are two different isoforms of this protein: a spliced form containing 206 amino acids (sp1) and an unspliced form with 209 amino acids (us) (Murata et al., 2006). The sp1 form is more abundant and is found in almost all ATL patients (Satou et al., 2006). Spliced HBZ is more potent than unspliced HBZ in inhibiting transcription from viral 5′ LTR. Indeed, experiments using cells transfected with tagged HBZ have shown that HBZ interacts with CREB-2 via its bZIP domain resulting in strong inhibition of the CREB-2/Tax-1 interaction instrumental for the activation of HTLV-1 LTR (Figure 5).

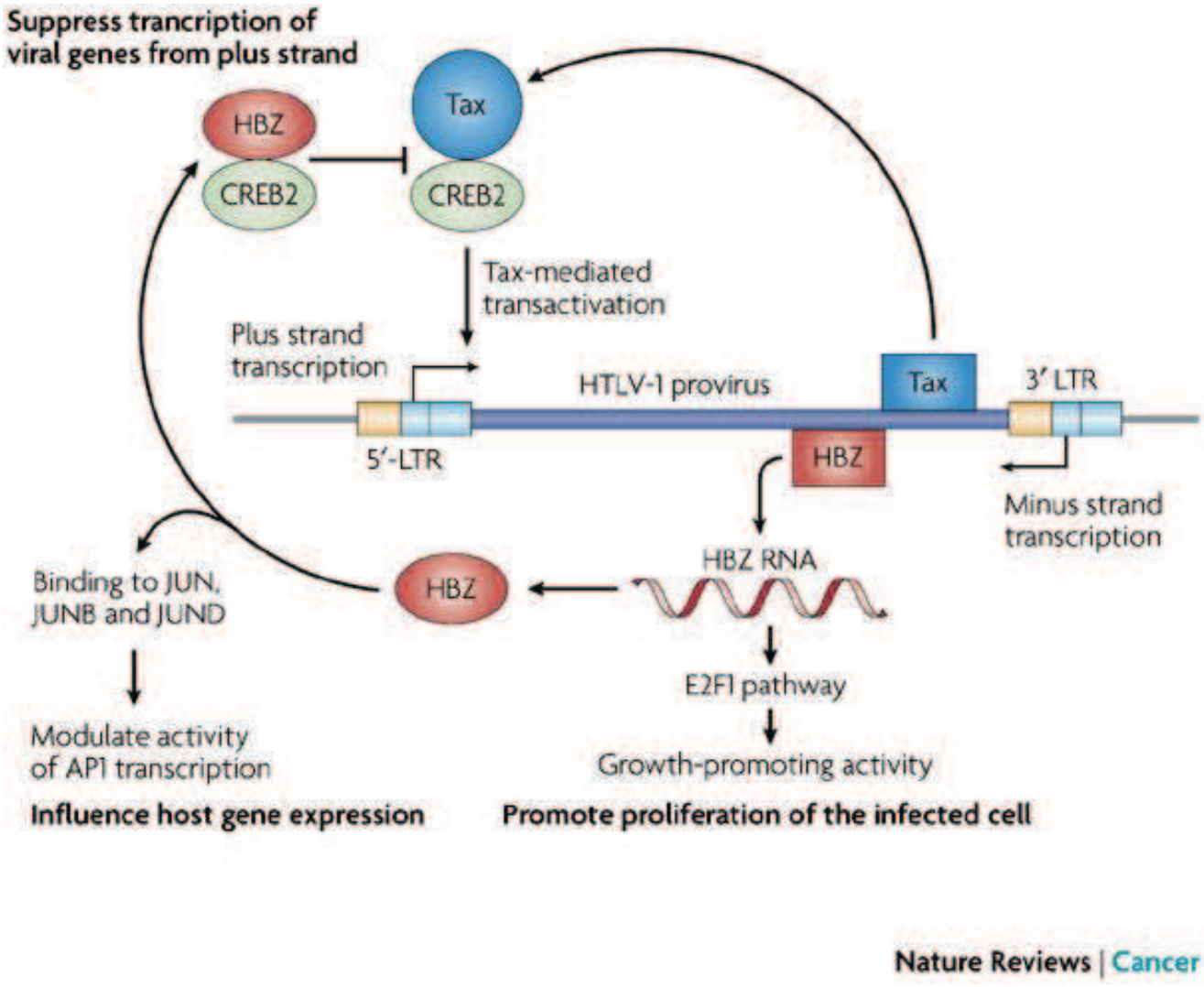

Figure 5. Schematic illustration of the expression and the activities of the HBZ RNA and protein in HTLV-1-infected cells. The effect of HTLV-1 basic leucine zipper factor (HBZ) on CREB2 and activating protein 1 (AP1) are shown. The effects of HBZ RNA on the E2F1 transcription factor and downstream E2F1-responsive genes are also shown. Current evidence suggests that the HBZ protein might antagonize the positive transcriptional effect of Tax on the HTLV-1 (human T-cell leukemia virus type 1) long terminal repeat (LTR). CREB, cyclic AMP responsive element binding protein (Matsuoka and Jeang, 2007)

In addition to interacting with CREB-2, similar experiments have shown that HBZ binds to different proteins of the JUN family via its bZIP domain (Basbous et al., 2003). The binding to JunB and cJun induces a sequestration of these factors in nuclear bodies or an accelerated degradation of them. As a result, HBZ reduces the cJun/JunB-mediated transcriptional activation of a series of genes. Conversely, the binding of HBZ to JunD does not inhibit the JunD-mediated transcriptional activation of target genes; indeed HBZ-JunD complex upregulates even the expression of HBZ encoding gene (Gazon et al., 2012). Interestingly, in many cases HBZ exerts opposite effects with respect to Tax-1 on signaling pathways (Matsuoka and Yasunaga, 2013). HBZ interacts with the KIX domain of p300/CBP to deregulate their interaction with cellular factors. This interaction strongly affects also the Tax-1-dependent, p300/CBP-mediated viral transactivation (Clerc et al., 2008). HBZ inhibits, while Tax-1 activates, the classical Nuclear Factor kappa B (NFkB) pathway by inducing PDLIM2 expression which brings about proteasomal degradation of RelA. HBZ suppresses, while Tax-1 activates,Wnt pathway by interacting with the disheveled-associating protein with a high frequency of Leucine residues (DAPLE) (Ma et al., 2013). HBZ inhibits production of Th1 cytokines (particularly IFN-γ) by interacting with NFAT and thus impairing cell-mediated immunity (Sugata et al., 2012). A number of effects suggest an important action of HBZ in supporting and/or maintaining the proliferation of HTLV-1 infected cells and by this the initiation and persistence of ATL. For example, the interaction of HBZ with JunD activates the telomerase by up-regulating the expression of hTERT (Kuhlmann et al., 2007).

HBZ interacts with ATF3 and reduces the interaction of ATF3 with p53, possibly interfering with p53 signaling leading to apoptosis and thus increasing the potential of ATL cells to proliferate (Hagiya et al., 2011).

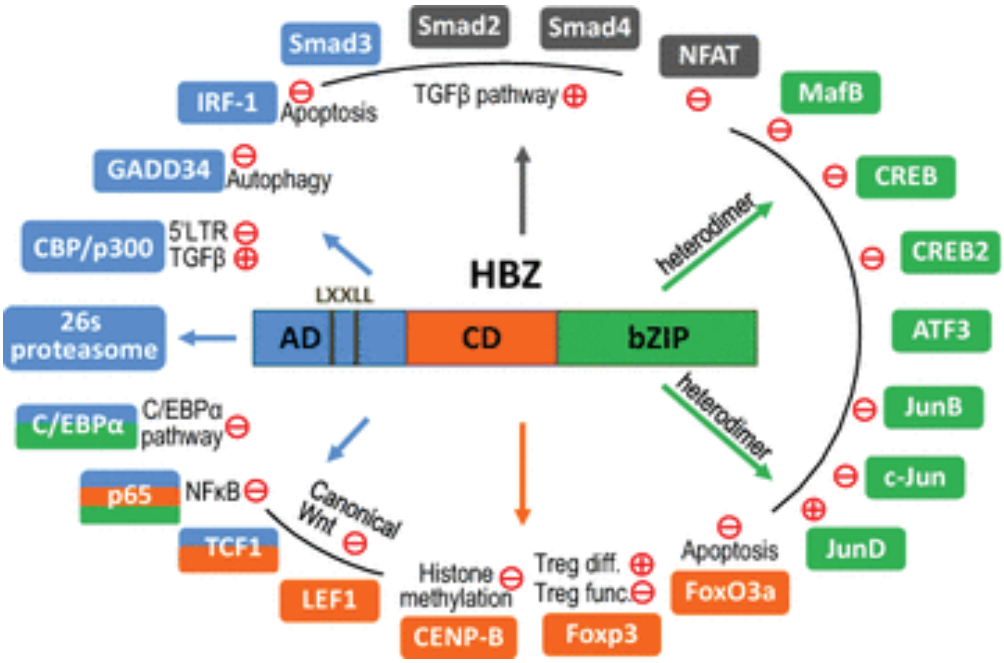

Figure 6. Cellular proteins that interact with HBZ. The three domains of sHBZ corresponding to the AD, CD or bZIP domains, are portrayed as squares in three different colors while the cellular binding partners of HBZ are shown as rectangles with colors corresponding to the various HBZ domains they interact with. Cellular proteins that bind to more than one domain of HBZ are painted in multiple colors whereas those lacking such information are painted in dark grey. The major pathways that these interactions have impact on, either positive (+) or negative (−), are noted close to respective cellular proteins. (Ma et al., 2016)

HBZ interacts with Smad3 and C/EBPα in a ternary complex which suppresses C/EBPα signaling pathway, again favoring proliferation of ATL cells. Moreover, the capacity of HBZ to participate in ternary complexes with Smad3 and its interacting factors, such as p300, may explain the up-regulation of TGFβ signaling pathway that is activated by Smad3-p300 (Figure 6). Interestingly TGFβ may increase the expression of FoxP3, a marker of regulatory T cells (Tregs) which can be infected by HTLV-1 (Zhao et al., 2011); this may predispose to the onset of ATL since the

$CD4^+Foxp3^+$ Treg cell phenotype has been found in ATL leukemic cells (Karube et al., 2004) although this aspect is still controversial (Toulza et al., 2009).

2 AIM OF THE STUDY

The aim of my study was to investigate in detail the expression and subcellular localization of endogenous HBZ protein in the context of HTLV-1 infected patients and particularly in those who evolved toward the HTLV-1 associated disease HAM/TSP. Most of the studies related to HBZ have been performed to date in HBZ-transfected cells that, for their nature, express HBZ protein in non physiological manner. This raises the possibility that the results obtained might bear limited biochemical and functional relevance. Only recently, by the use of the first reported monoclonal antibody against HBZ, 4D4-F3, generated in our laboratory it was possible to investigate for the first time the expression and the biochemical interaction with host factors of endogenous HBZ in HTLV-1 chronically infected cells, in ATL cell lines and, most importantly in fresh PBMCs of an ATL patients. The present work was set to determine whether I could detect and define by confocal microscopy the subcellular localization of endogenous HBZ in HAM/TSP. Moreover, the analysis was extended to more cases of ATL and to infected asymptomatic carriers (AC). In addition, by taking advantage of an immortalized CD4+ T cell line purified from HAM/TSP patient, we started to analyze the biological basis of the HBZ oncoprotein expression in a cellular model of HAM/TSP disease.

3 MATERIALS AND METHODS

3.1 Cells

Human embryonic kidney 293T cells (kindly provided by Prof. B.M. Peterlin, UCSF, San Francisco, USA) were cultured in Dulbecco's modified Eagle medium (DMEM) containing 5 mM L-glutamine and supplemented with 10% fetal calf serum (FCS).
ATL-2s is a T cell line derived from a leukemic patient kindly provided by Dr. Matsuoka, Japan (Takeda et al., 2004). Cells were maintained in RPMI-FCS 10%.
Peripheral blood monuclear cells (PBMC) from healthy donors, HTLV-1+ asymptomatic carriers, HAM/TSP patients were purified by Ficoll-Paque TM PLUS (GE-Healthcare Bio-Science, Milan, Italy) of heparinated blood. PBMC from healthy donors were obtained by the Blood Transfusion Center, Ospedale di Circolo, Fondazione Macchi, Varese, whereas PBMC of HTLV-1-infected patients were obtained through the Biomedical Research Program approved by the Committee for the Protection of Persons, Ile-de-France II, Paris (2012-10-04 SC). All PBMC preparations were immediately frozen at -80°C and subsequently transferred in liquid nitrogen after 48–96 hours. The two ATL patients analyzed in this study, PH1393 and PH1505, were suffering from a typical acute ATL form characterized by high hyperlymphocytosis with lymphocyte count of 18.000/mm^3 and 30.000/mm^3, respectively, and with 79% and 80% of atypic lymphocytes, as evaluated by optical microscopy. Chronically HTLV-1-infected CD4_ T-cell line (CIB) (kindly provided by Dr. Claudine Pique_Institut Cochin. Paris, France) were generated by long-term culture in the presence of IL-2 of CD4+ T cells isolated from blood samples collected from a HAM/TSP patient (Ozden et al., 2004) . Chronic HTLV-1 expression was monitored by indirect immunofluorescence.

3.2 Transfection and treatments

Plasmid encoding myc-tagged HBZ was a gift of Dr. Matsuoka, Univ. of Kyoto, Japan. Plasmid encoding Tax-1 was previously described (Tosi et al., 2011). 293T cells were cultured on glass coverslips pre-coated with poly-L-lysine placed in 24 well plates. Cells were transfected with 0.2 μg of each plasmid by using FuGENE HD (Promega, Milan, Italy) in a ratio 3 μl/μg DNA. Cells were incubated with the transfection mixture until processed for confocal microscopy. Where indicated, the 293T cells or HAM/TSP PBMC were incubated with 20 nM leptomycin B (LMB; Sigma) or the vehicle methanol for 3 h at 37°C, 5% CO2.

3.3 Immunofluorescence and confocal microscopy

Frozen vials containing PBMC were thawed by immediate passage from liquid nitrogen to a water bath set at 37°C. Cells were washed with warm RPMI medium and processed for immunofluorescence and confocal microscopy.

For confocal microscopy, appropriate number of cells were cultured on glass coverslips pre-coated with poly-L-lysine (0.1gr/ml, Sigma) for five hours. The cells were then washed with 1x PHEM buffer, pH 6.9 (60 mM PIPES, 25 mM HEPES, 10mM EGTA, 2mM MgCl2) three times, fixed in methanol 7 minutes at -20°C, and blocked with 1% BSA in 1x PHEM for 1h at room temperature (RT). Cells were then stained overnight with anti-HBZ 4D4-F3 monoclonal antibody (mAb), anti-Tax-1 mAb (clone 168 A51-2 from the NIH AIDS Research and Reference Reagent Program), anti-vimentin rabbit polyclonal antibody (Santa Cruz Biotechnology, CA, USA), anti-CD4 rabit monoclonal antibody (clone EPR6855, ABCAM) and anti-CD19 rabbit monoclonal antibody (clone EPR5906, ABCAM), diluted in PHEM buffer containing 0.5% BSA. The slides were then washed five times with cold 1x PHEM and incubated in the dark for 2h at RT with the following secondary antibodies from Life Technology (Waltham, MA USA): goat anti-mouse IgG1 coupled to Alexa Fluor 546 to detect HBZ, goat anti-

mouse IgG2a conjugated to Alexa Fluor 488 to detect Tax-1, and goat anti-rabbit IgG conjugated to Alexa Fluor 488 or to Alexa Fluor 546 to detect vimentin, CD4 or CD19. For co-staining with directly labelled antibodies, after extensive washing with 1x PHEM, anti-CD8 rabbit monoclonal antibody directly conjugated to Alexa Fluor 647 (clone EP1150Y, ABCAM) and mouse anti-human CD25 monoclonal antibody directly conjugated to Alexa Fluor 488 (clone BC96, BioLegend) were added after the indirect immunofluorescence for two hours at room temperature. Similarly, after indirect immunofluorescence, the nuclei were stained by incubating the cells with DRAQ5 Fluorescent Probe (Thermo Scientific, Waltham, MA USA), for 30 min at room temperature. After washing, the slides were mounted on coverslips with the Fluor Save reagent (Calbiochem, Vimodrone (MI), Italy) and examined by a confocal laser scanning microscope (Leica TCS SP5; HCX PL APO objective lenses, 63x original magnification, numerical aperture 1.25). Images were acquired and analyzed by LAS AF lite Image (Leica Microsystem, Milan, Italy) and/or Fiji (Image J) softwares.

3.4 Flow Cytometry Analysis

Frozen vials containing PBMC were thawed by immediate passage from liquid nitrogen to a water bath set at 37°C. Cells were washed with warm RPMI medium and immediately processed for flow cytometry analysis with the BD FACSAria II™ apparatus. The following reagents were used: mouse anti-human HLA class I (clone B9.12); mouse anti-human HLA class II DR (clone D1.12), both revealed by FITC-labelled rabbit anti-mouse IgG F(ab')2 antiserum (Sigma, Milan, Italy); FITC mouse anti-human CD3 (clone (UCHT1, BD Pharmingen); FITC mouse anti-human CD4 (clone RPA-T4, BD Pharmingen); PE-Cy5 mouse anti-human CD8a (clone RPA-T8; eBioscience, Milan, Italy); PE mouse anti-human CD16 (clone B73.1, eBioscience, Milan, Italy); FITC mouse anti-human CD19 (clone HIB19, BD Pharmingen) and phyco-erythrin (PE) mouse anti-human CD25 (clone M-A251, BD Pharmingen). Rendering and imaging were performed with FlowJo software (Version 7.6.5).

3.5 cDNA synthesis and QRT-PCR

Total RNA was extracted from one million cells using Trizol (Invitrogen, Carlsbad, USA) and cDNA synthesized from 0.5 μg RNA by using Iscript (Bio-Rad) according to the manufacturer's protocol. PCR reactions were performed with an ABI Prism 7900 HT Sequence Detection System by using 5 μl of each diluted RT sample (10 ng/μl) and 20 μl of diluted Taqman Universal PCR Master Mix (Applied Biosystems); each reaction was performed in duplicate. The cycling conditions comprised an initial step at 50°C for 2 min, denaturation at 95°C for 10 min, and 40 cycles at 95°C for 15 sec and 60°C for 1 min. The following primers were used for amplifying HBZ SPLICED1 and HBZ UNSPLICED transcripts:

HBZ-UNSPLICED-FW	GCGGATCCATGGTTAACTTTGTATCT
HBZ-UNSPLICED-RW	GCGAATTCTTATTGCAACCACATCGCCTC
HBZ-SPLICED1-FW	GCGGATCCATGGCGGCCTCAGGGCTG
HBZ-SPLICED1-RW	GCGAATTCTTATTGCAACCACATCGCCTC

The Ct values were calculated by using standard curves constructed from 5-fold serial dilutions of a plasmid containing the Glyceraldehyde 3-phosphate dehydrogenase (GAPDH) amplicon, or HBZ amplicon. The absolute copy number of each transcript was determined and normalized for the copy number of the GAPDH.

3.6 SDS/PAGE and Western Blotting

293T, 293T myc-HBZ transfected, ATL and CIB cells were collected and lysed with lysis buffer containing 1% NP-40, 10mM Tris-Hcl pH 7.4, 150nM Nacl, 2mM EDTA, 1uM phenylmethylsulfonyl fluoride (PMSF) and protease inhibitors cocktail (sigma). Cell debris were removed by centrifugation at 14.000 rpm for 10 minutes at 4 °C and

the supernatant were collected. Cell Lysate were analysed for the expression of HBZ protein in denaturating conditions by gel electrophoresis followed by western blotting. For the denaturating gel electrophoresis the lysates were diluted with 6x SDS-sample buffer (0.3M Tris-Hcl pH 6.8, 0.6 M DTT, 10% SDS, 0.6% bromophenol blue, 60% glycerol) and boiled for 3 minutes before loading on the gel. Protein were than separated by electrophoresis on 8% polyacrylamide gel containing 0.1% SDS and transferred into a nitrocellulose membrane (Amershamk Protran Premium 0.45 micron NC, Ge Healtcare) by electroblotting (360 mA for 1h) at 4 degrees. After blocking with 5% non-fat dry milk in PBS for 1h at room temperature, the membrane was incubated with the primary antibody diluted in 5% non-fat dry milk in PBS, overnight at 4 °C under continuous agitation. The membrane was than washed three times for 10 minutes with PBS and than incubated with the secondary antibody solution (HRP-conjugated goat anti mouse secondary antibody) for 2h at room temperature, under agitation. After 3 washes with PBS, blots were developed by ECL (Supersignal West pico chemiluminescent substrate, Thermo Fisher Scientific).

3.7 Immunoprecipation

For immunoprecipitation 10 millions of CIB, ATL cells and 3 million untransfected or myc-HBZ-transfected 293T cells were lysed on ice for 50 minutes with IP lysis buffer containing 1% NP-40, 10mM Tris-Hcl pH 7.4, 150nM Nacl, 2mM EDTA, 1µM phenylmethylsulfonyl fluoride (PMSF) and protease inhibitors cocktail (Sigma). Cell lysates were centrifuged at 14000 rpm for 10 minutes and the supernatant were pre-cleared with protein A Sepharose fast flow beads (GE Healtcare) for 30 minutes at 4 degrees by rotation. To precipitate HBZ protein, after pre clearing, the cleared lysates were incubated with 1ug of anti-HBZ antibody (4D4-F3) for 1h on ice and then reacted with 50µl of protein A beads overnight at 4 degrees by rotation. The immune

precipitated proteins were analyzed by western blots using anti-HBZ monoclonal antibody.

3.8 Immunohistochemistry

Immunohistochemical studies were performed on 3µm formalin-fixed, paraffin-embedded sections following standard procedures. Antigen retrieval was performed with a 10 min microwave treatment in 10 mM Citrate Buffer (pH 6) and after washing in TBS Triton Buffer (pH 7.4). Sections were incubated overnight at 4°C with the 4D4-F3 anti-HBZ monoclonal antibody (1:1000 dilution of ascitic fluid). The sections were then incubated with biotinilated goat anti-mouse antibody for 2 h (Vector Laboratories, Burlingame, CA, USA) followed by ABC-peroxidase complex (Vector Laboratories) according to manufacturer's protocol. The immunoreaction was developed with 3.3'-diaminobenzidine tetrahydrochloride (DAB) (Sigma Aldrich, St. Louis, MO, USA) as chromogen. Nuclei were counterstained with Harris hematoxylin and finally sections were dehydrated and embedded in Pertex (Kaltek Srl, Padua, Italy).

4 RESULTS

4.1 Phenotypic features of ATL cells and expression of HTLV-1 HBZ protein in PBMC of ATL patients

To expand previous studies performed in this laboratory in ATL patients (Raval et al., 2015), PBMC of two patients, PH1393 and PH1505, were investigated for the expression of cell surface markers by immunofluorescence and flow cytometry and for the expression of HBZ by immunofluorescence and confocal microscopy.

Results of cell surface phenotype are shown in Figure 7. Patients exhibited a surface phenotype of a T cell leukemia. (Figure 7). Indeed most of the cells were leukemic and expressed the CD4 marker. Interestingly, cells from patient PH1383 expressed high level of the CD25 T cell activation marker in a homogenous fashion, overlapping the cells with the CD4+ phenotype. CD25 marker was expressed at very low level, instead, in the PH1505 patient cells. Of note, while in PH1393 all cells were CD3 positive, PH1505 was negative for CD3. The cells of both patients were negative for CD8, CD16 and CD19 surface markers.

When the patients' cells were analyzed for expression of HBZ, 80% and 83% of the cells from patient PH1393 and PH1505, respectively, were positive for HBZ (Table 1). HBZ was localized in speckle-like structures in the nucleus **(**Figure 8**)**. Parallel staining for the nuclear marker DRAQ5, and for the cytoplasmic marker vimentin, confirmed the exclusive nuclear localization of HBZ. PBMC of the two ATL patients were also analyzed for the presence of Tax-1 protein; none of them showed positivity for this viral protein (Table 1).

4.2 Tax-1 but not HBZ is expressed in PBMC of asymptomatic carries.

PBMC from the three asymptomatic carriers (AC), namely PH1614, PH1619 and PH1621, were similarly analyzed for their cell surface phenotype (Figure 9) and for the intracellular expression of HBZ and Tax. Flow cytometric analysis indicated in certain patients limited differences in the expression of relevant lymphocyte subpopulation markers with respect to normal PBMC cells used as controls. An appreciable difference was in the expression, but not the proportion, of the CD4 cell marker, which was consistently reduced in all three AC. The significance of this finding will require further assessment in a higher number of cases.

Interestingly, the PBMC of all three AC did not show any positivity for HBZ, when analyzed by immunofluorescence and confocal microscopy (Figure 10A), although they expressed Tax-1 in a small but distinctive proportion of cells: 11%, 1% and 6%, respectively (Table 1) with a preferential, although not exclusive, nuclear localization (Figure 10B).

4.3 Cytoplasmic localization of HTLV-1 HBZ protein in PBMC of HAM/TSP patients

In order to define the subcellular localization of endogenous HBZ in HAM/TSP, PBMC of four HAM/TSP patients, namely PH1485, PH1593, PH1601 and PH1624 were studied by cells surface marker analysis, immunofluorescence and confocal microscopy analysis.

When analyzed for relevant lymphocyte cell markers, all patients exhibited a cell surface expression similar to the one expressed by normal PBMC (Figure 11).

Of particular relevance, instead, and in striking contrast with the HBZ nuclear localization in ATL (Raval et al., 2015), all four HAM/TSP patients presented an HBZ localization confined exclusively to the cytoplasm (Figure 12A) (Baratella et al., 2017).

Parallel staining with DRAQ5, a nuclear marker, and with vimentin, a cytoplasmic marker, confirmed this exclusive HBZ cytoplasmic localization. HBZ appeared as discrete dots, similar in shape to the nuclear speckles found in PBMC of ATL patients. The percentage of HBZ positive cells was comprised between 4 to 11% of total PBMC in three of the four patients analyzed with the exception of patient PH1601 having only 0,4% HBZ-positive cells (Table 1). PBMC from HAM/TSP patients were then analyzed for the expression and subcellular localization of Tax-1 protein. Tax-1 was expressed in 1%, 14% and 20% of the PBMC of PH1601, PH1485 and PH1624 patients, respectively (Table 1). Tax-1 was undetectable in PH1593 PBMC. In patient PH1485 Tax-1 was localized in dot-like structures in the nucleus **(**Figure 12B**).** A proportion of these cells expressed Tax-1 also in the cytoplasm. In patient PH1624 PBMC, Tax-1 was localized in the nucleus with a large proportion of these cells expressing Tax-1 also in the cytoplasm. Importantly, in this restricted series of patients, no cells were found to co-express HBZ and Tax-1 (Figure 12C).

4.4 HBZ in HAM/TSP stably resides in the cytoplasm and does not shuttle to and from the nucleus

In order to assess whether the cytoplasmic localization of HBZ in PBMC of HAM/TSP patients is a stable feature or dynamic event resulting from a rapid recycling of the protein from the nucleus, PBMC from PH1624 patient were treated with Leptomycin B (LMB), an inhibitor of Cmr1-dependent nuclear export, and analyzed by immunofluorescence and confocal microscopy. Results clearly indicate that the HBZ cytoplasmic localization in PBMC of HAM/TSP was not affected by LMB treatment **(**Figure 13A). Conversely, as was previously shown in our laboratory (Forlani et al., 2016) this treatment resulted in a prominent nuclear retention of Tax-1 protein in 293T cells transfected with a Tax-1-expression vector **(**Figure 13B**).** From these results, we conclude that in HAM/TSP patients, HBZ is specifically retained into the cytoplasm and does not shuttle into the nucleus throughout the exportin-dependent nuclear export.

4.5 HBZ-positive cells in HAM/TSP representative PH1624 patient are found in the CD4+/CD25- T cell subpopulation

In order to define the cellular subpopulation expressing the cytoplasmic HBZ protein in HAM/TSP patients, we analyzed in detail the PBMC of patient PH1624 displaying one of the highest number of HBZ-positive cells (9%). Analysis of cell surface markers by immunofluorescence and flow cytometry showed that this patient expressed CD3, CD4 and CD8 markers in 88%, 63% and 27% of PBMC, respectively. This phenotype was very similar to the one of PBMC from a normal donor. Interestingly the T cell marker CD25, known to be expressed in activated as well as in regulatory T (Treg) cells was not detected in PH1624 PBMC (Figure 11), whereas it was expressed at low amount in 4–5% of normal PBMC. The B cell compartment, as assessed by the

presence the CD19 marker, was represented in almost equal proportion of PH1624 (10%) and normal (8%) PBMC. NK cells, as assessed by the CD16 marker, were 4% of PH1624 PBMC and 10% of normal PBMC. HLA class I was expressed in 100% of both PH1624 and normal PBMCs, and HLA class II was expressed in 15% and 18% of PH1624 and normal PBMC, respectively (Figure 11).

Subsequently, confocal microscopy analysis was performed. Cytoplasmic HBZ was clearly detected in a significant proportion of CD4+ cells (Figure 14A). Indeed, 15% of CD4+ T cells were also HBZ positive. Considering that cytoplasmic HBZ was detected in 9% of the total PBMC of PH1624 patient, and that CD4+ T cell represented around 63% of the PBMC in this patient, it derives that virtually all HBZ+ cells are included in CD4+ T cell compartment. Cytoplasmic HBZ+ cells were virtually not detected in the CD8+ PBMC of PH1624 patient (Figure 14B). In fact, after careful analysis of more than one hundred CD8+ T cells, only one cell was found to co-express HBZ in its cytoplasm (Figure 14B). Confocal analysis of CD25 expression in PH1624 patient's PBMC confirmed that cells were negative for this marker (Fig. 15). Similarly, neither CD19+ B cells nor CD16+ NK cells were found to express cytoplasmic HBZ. Thus, in a representative HAM/TSP patient displaying a high percentage of HBZ-positive cells, cytoplasmic HBZ is almost exclusively found in $CD4^+$ T cells and these cells do not co-express the CD25 marker.

4.6 HBZ and Tax-1 expression in the HAM/TSP patient cell line CIB

To confirm and better understand the peculiar distribution of the HBZ oncoprotein in the HAM/TSP pathology we took advantage of an immortalized CD4+ T cell line, designated CIB, obtained by continuous culturing in IL-2 of purified CD4+ T cells isolated from PBMC obtained from an HAM/TSP patient (Ozden et al., 2004).

By immunohistochemistry and light field microscopy we assessed the distribution of the HBZ oncoprotein in this cells line with our 4D4-F4 anti HBZ antibody (Figure 16). Virtually all cells expressed HBZ and again the expression seemed to be confined to the cytoplasmic compartment. This finding was confirmed by more refined confocal microscopy analysis as it is shown in Figure 17.

Biochemical experiments were then set up to assess the comparative amount of HBZ expressed in the CIB cell line with respect to the adult T cell leukemia-derived cell line ATL-2 (Figure 18). indicate that the degree of HBZ expression in the two cell lines was similar, although CIB cell line expressed an additional band of 20 kDa related to HBZ whose molecular nature is presently under investigation. Interestingly, and as previously shown (Raval et al., 2016) the total amount of endogenous HBZ expressed in either ATL-2 or CIB cell lines was much lower than the amount expressed in HBZ-transfected 293T cells further emphasizing the notion that the conclusions derived from biochemical and functional correlates found in HBZ-transfected cells should be carefully reconsidered and framed in the context of endogenously expressing HBZ-positive cells.

CIB cells were subsequently analyzed for the expression of the HTLV-1 Tax-1 oncoprotein as well. Interestingly, careful analysis by confocal microscopy of Tax-1 expression in CIB cells showed that only 30% of the cells were positive for the viral protein (a representative Tax-1-positive cell is shown in Figure 19). Tax-1 displayed the characteristic speckle-like aspect and the localization was mostly cytoplasmic with few spots in the nucleus. Nevertheless, this level of Tax-1 expression was sufficient to

activate the NF-kB pathway as shown by the nuclear translocation of NF-kB p65 (Figure 20).

Since most of Tax-1 was found localized in the cytoplasm, I further investigated the possibility that in those CIB cells co-expressing Tax-1 and HBZ, the two protein co-localized together. Confocal microscopy showed a clear distinct distribution of the two viral proteins in the cytoplasm, indicating that HBZ and Tax-1 do not interact each other in CIB cells (Figure 21).

4.7 Spliced-1 and Unspliced HBZ are both expressed in HTLV-1 infected asymptomatic carriers and in HAM/TSP patients.

As described in the Introduction, HBZ consists of two different forms derived from a spliced or an unspliced mRNA. In order to evaluate the possibility that a distinct splicing form could be implicated in the exclusive cytoplasmic distribution of HBZ protein found in HAM/TSP patients, RT-PCR of spliced and unspliced forms was carried out in mRNA preparations from PBMC of 7 HAM/TSP patients, 2 AC, as well as from CIB and ATL-2s leukemic cells.

The results depicted in Figure 22 indicate that both forms are expressed in the various cell samples analyzed including the 7 PBMC samples of HAM/TSP patients with a tendency of the spliced form to be more expressed in HAM/TSP samples although with no statistical significance. This difference is more pronounced in samples derived from the two asymptomatic carriers (AC) analyzed, although a more extensive number of cases should be analyzed before drawing conclusions on the real meaning of this finding.

5 DISCUSSION AND FUTURE PERSPECTIVES

Infection by HTLV-1 generally leads to a state of asymptomatic carrier which may last for the entire life. However, in 3–7% of individuals a very severe form of leukemia/lymphoma or a chronic progressive neurological disease can develop as result of the infection. The oncogenic progress leading to ATL has been mainly attributed to the viral transactivator Tax-1 that hijacks the basic mechanisms of control of cellular homeostasis (Giam and Semmes, 2016). Nevertheless, only 40% of ATL patients can express Tax-1 whereas all of them express HBZ, an event that has been interpreted as an involvement of Tax-1 in the first phases of oncogenic process and of HBZ in the maintaining of leukemic state (Matsuoka and Yasunaga, 2013). While recent data have unambiguously demonstrated the nuclear localization of endogenous HBZ in ATL cells and in chronically infected cell lines (Raval et al., 2015), no data were available on the endogenous expression and subcellular localization of HBZ in patients affected by HAM/TSP. My PhD thesis was focused particularly in assessing the expression and subcellular distribution of HBZ protein in PBMC of patients affected by the HAM/TSP disease and in comparing it to asymptomatic carriers and patients affected by ATL. I was able to demonstrate that a discrete percentage, up to 11%, of PBMC from HAM/TSP patients express HBZ and that this expression is exclusively confined to the cytoplasm. Cytoplasmic HBZ appears distributed in dots similar to the nuclear speckle-like structures observed in leukemic cells of ATL patients, sometimes dispersed all over the cytoplasm, sometimes concentrated in a restricted area of it (Baratella et al., 2017). This unprecedented finding was further confirmed by the study of an IL-2-dependent T cell line derived from a HAM/TSP patients, the CIB cell line, in which it was also possible to conduct additional preliminary biochemical analysis to compare the amount of HBZ expressed in HAM/TSP cells compared to ATL-2s leukemic cells. This analysis showed a similar expression in the two cell lines and further demonstrated the relatively much lower expression of endogenous HBZ as compared to the expression observed in HBZ-

transfected cells, as was previously observed in our laboratory (Raval et al., 2015). This finding should lead to caution in drawing conclusions related to the biochemical interaction of HBZ with other intracellular partners and consequent functional correlates of these interactions *in vivo* when these findings are obtained in transfected cells in which overexpression of HBZ may alter the interpretation of the data.

The exclusive cytoplasmic distribution of HBZ in PBMC of HAM/TSP patients was not due to a preferential shuttling of the protein from the nucleus to cytoplasm, since treatment of the cells with Leptomycin B, a drug that blocks the CRM1-dependent nuclear-cytoplasmic shuttling of the proteins, did not result in even partial segregation of the protein into the nucleus, strongly indicating that HBZ is a cytoplasmic resident, non migrating protein in HAM/TSP patients.

It has been recently described the existence of amino acid variations in the HBZ protein both in asymptomatic carriers and HAM/TSP patients, identified in the activation domain and in the nuclear localization signal sequence (Mota-Miranda et al., 2013). Thus it might be possible that HBZ sequence variation may influence the subcellular localization of the protein. However, this should not certainly involved a possible exclusive expression of either one of the two major forms of HBZ described, that is the unspliced and the spliced form, as both mRNAs of these forms were present in cells of HAM/TSP patients, as well as in cells of leukemic patients. Thus other mechanism should be responsible of the exclusive cytoplasmic distribution of HBZ in HAM/TSP. Future studies on possible partner interactors of HBZ in the cytoplasm will certainly help in clarifying this aspect.

An additional interesting finding reported in the present study concerns the expression and localization of HTLV-1 Tax-1 at the single cell level. In PBMC of HAM/TSP patients, when detectable, Tax-1 was localized mostly in the nucleus and in a variable proportion of the cells in both nucleus and cytoplasm. Importantly, it was never expressed in the same cells expressing HBZ. While uncoupling of Tax-1 and HBZ expression is rather common in ATL patients (Matsuoka and Jeang, 2007; Takeda et al., 2004),(Satou et al., 2006) , the mutually exclusive expression of either HBZ or Tax-

1 proteins at the single cell level has never been reported. The molecular basis of this event in cells of HAM/TSP patients is unknown at present, and certainly will be the focus of our future investigation. It is tempting to speculate that this finding may be relevant at the functional level and particularly in the immune recognition of HTLV-1 infected cells. The HBZ cytoplasmic localization, possibly in extra-endosolic compartments, may not be appropriate to the generation of peptides that can efficiently bind MHC class I molecules for presentation to, and scrutiny by cytotoxic T cells (CTLs). This may explain the relatively low level of HBZ-specific CTLs in HAM/TSP (Macnamara et al., 2010) in conjunction with the unsatisfactory lytic efficiency of HBZ-specific CTLs with respect to the strong recognition and lytic efficiency of Tax-1-specific CTLs (Hilburn et al., 2011). A note of caution, however, should be expressed in relation to the mutually exclusive expression of HBZ and Tax-1 in HAM/TSP disease. Indeed the model cell line CIB derived from a patient with HAM/TSP was found to coexpress HBZ and Tax-1. The reason of this striking different aspect of CIB with respect to fresh PBMCs is at present under investigation. A possible explanation could be that *in vitro* growing of CIB may have altered the pattern of expression and subcellular distribution of Tax-1 in a cell that at the origin did not express Tax-1 at all. Alternatively, CIB is indeed one of those very few cells that co-expressed HBZ and Tax-1 from the beginning and for this reason may have had growth advantage in culture when isolated from the patient. Whatever the mechanism underlying this event, it was clear from the data presented in this thesis that HBZ and Tax-1 did not co-localize in the same speckles and thus they could not significantly interact each other.

Additional confocal microscopy analysis of PBMC of a representative HAM/TSP patient PH1624 clearly showed that the major, if not the exclusive, HBZ+ cell subpopulation was represented by CD4+ cells. After counting a large number of CD8+ PH1624 cells, only 1 was found to express cytoplasmic HBZ. Thus, if from one side this result indicates that CD8+ cells can be infected by HTLV-1 and express HBZ in the HAM/TSP patients, this event is extremely rare as compared to the frequency of HBZ+/CD4+ cells. PBMC of HAM/TSP patient PH1624 did not reveal the presence

of CD25+ T cells by FACS analysis. Further refinement by confocal microscopy analysis confirmed the absence of CD4+/CD25+ T cells, a subset that includes regulatory T cells (Treg). Although CD4+/CD25+ Tregs can be infected by HTLV-1 and HAM/TSP patients have been shown to have a high number of CD4+/CD25+ Tregs with impaired function (Araya et al., 2011) as well as HBZ mRNA expression levels comparable to those observed in ATL (Yamano et al., 2009), our result indicate that in HAM/TSP patients HBZ protein expression can be easily found in CD4+ T cells not displaying the classical phenotype of Treg cells. Additional studies are certainly required to further detail the phenotype and the functional correlate of CD4+ T cells expressing HBZ protein in HAM/TSP patients.

In conclusion, based on the results presented in this Thesis, we propose that HBZ cytoplasmic localization can be considered as a *bona fide* biomarker of HTLV-1-derived HAM/TSP pathology.

Although several studies have been focused at clarifying the role of HBZ in HTLV-1-associated diseases, much research is still required to clearly define the involvement of HBZ in the molecular and cellular events that lead to the distinct outcome of viral infection, whether evolving versus the leukemia/lymphoma or versus the neuroinflammatory disorders.

The discovery of HBZ has led to important new research avenues with potential association with HTLV-1-associated diseases (Barbeau et al., 2013). In fact, ATL cells from infected patients consistently express HBZ and substantial evidence points toward HBZ implication in viral persistence and ATL cell survival. Our evidences further suggest that HBZ in the cytoplasmic compartment can represent a potential marker of a different pathological state, namely HAM/TSP. Several cellular factors are known to interact with HBZ, and it will be extremely important to analyze such interactions in the context of HAM/TSP and comparing them to the ones in ATL disease, in relation to the different cellular localizations HBZ protein. These comparative studies will provide a better understanding as to the mechanism by which

HBZ is involved in HAM/TSP development, which might also lead to new potential HAM/TSP treatment.

With the above limitations in mind, the cumulative studies presented in this thesis suggest, however, a possible roadmap in the evolution of HTLV-1 infection (Figure 23). We may think that primary HTLV-1 infection is characterized by the expression of Tax-1 (this stage may be observed in PBMC of still asymptomatic patients), followed by the possible transient co-expression of HBZ (yet to be demonstrated). As we have no specific demonstration of this intermediate step, we do not know whether HBZ protein can localize in the nucleus, cytoplasm or both cellular compartments at these early stages of infection. Immediately after, a compartmentalization of HBZ in the cytoplasm can take place in case of evolution of the infection towards HAM/TSP. At this stage, the evolving pathology can either present a concomitant Tax-1 expression in the same cells (the CIB cell may represent one of these cases), or a mutually exclusive expression of Tax-1 and HBZ in different cells, as we observed in our patients. Conversely, in case of evolution toward the leukemic stage, HBZ will be expressed always and only in the nucleus with or without the co-expression of Tax-1. This hypothetical scheme is useful to test several additional hypotheses and investigate previously unforeseen mechanisms. For example, can we hypnotize a stage in which HBZ is compartmentalized in the cytoplasm still without clinical signs of neurological disease and use this parameter also as a prognostic marker of future development toward HAM/TSP. Moreover, we believe, that now we can experimentally investigate what are the molecular mechanisms that drive the distinct nuclear or cytoplasmic localization of the HBZ protein, the specific interactors that retain HBZ in the two different cellular compartments and if are these mechanisms related to the onset and/or the persistence of the distinct pathologies.

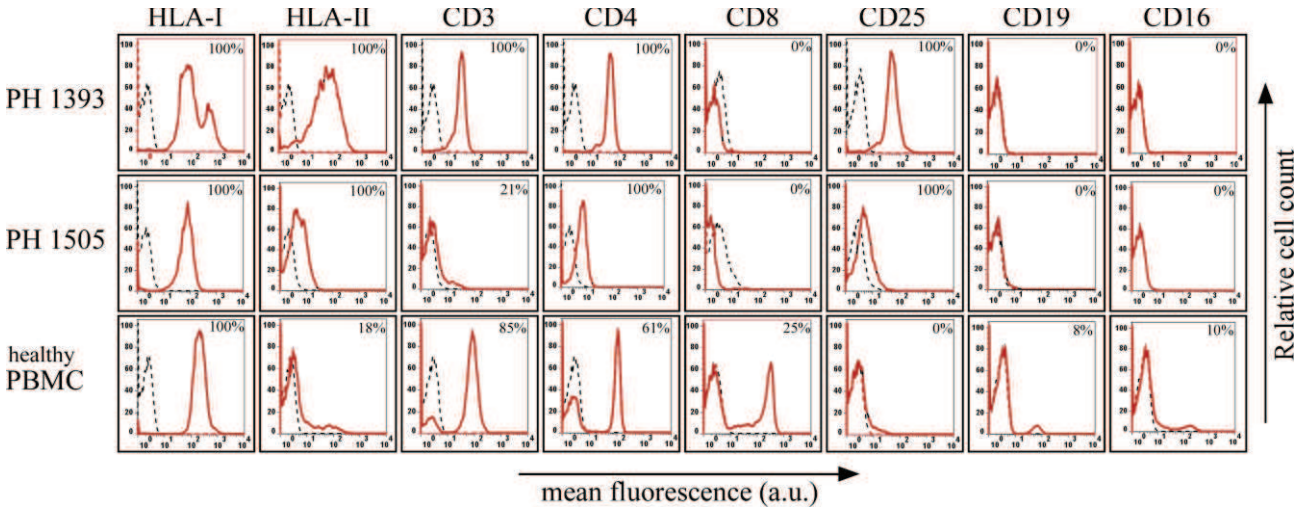

Figure 7. Expression of cells surface markers in PBMC of ATL patients PH1393 and PH 1505 and healthy control. The expression of HLA class I, HLA class II DR, CD3, CD4, CD8, CD25, CD19, and CD16 surface molecules on PBMC from ATL patient PH1393, 1505 and a healthy control was assessed by immunofluorescence and flow cytometry with antibodies specific for the various markers. Results are expressed as relative number of cells (ordinate) versus the mean intensity of fluorescence in arbitrary units (abscissa). In each histogram, negative controls, obtained by staining the cells with an appropriate isotype-matched antibody, are depicted as dashed line. The percentage of positive cells for the cell surface marker analyzed are indicated on the top right of every panel.

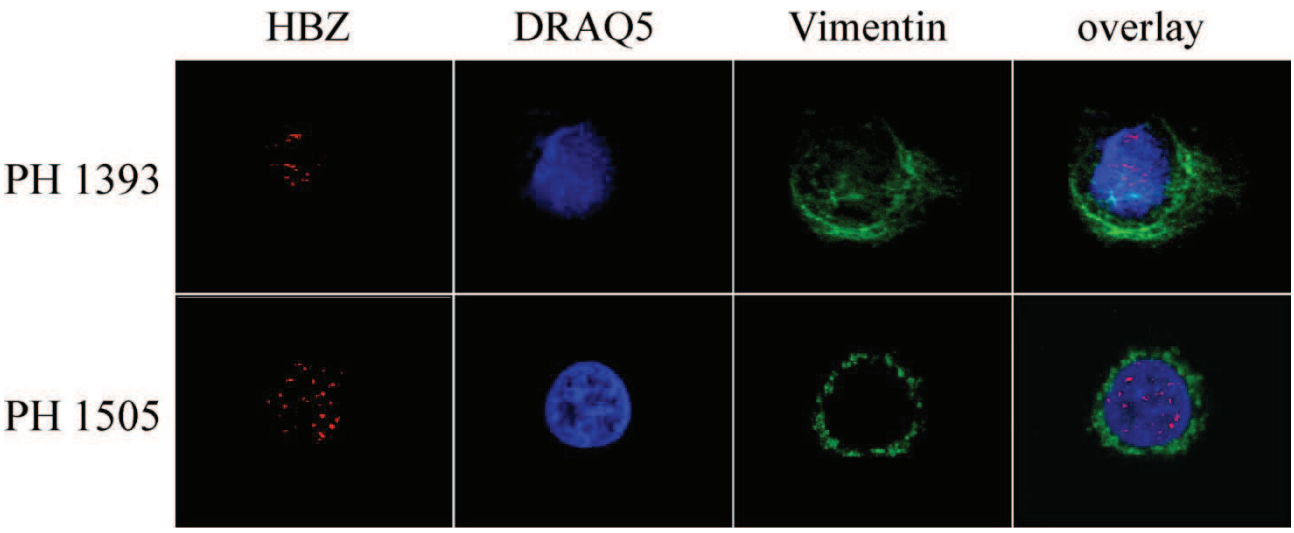

Figure 8. Subcellular localization of endogenous HBZ and Tax-1 in PBMC of ATL patients. PBMC of two ATL patients (PH1393 and PH1505) were stained with the anti-HBZ 4D4-F3 mAb, followed by Alexa Fluor 546-conjugated goat anti-mouse IgG1antibody to detect the HBZ protein and analyzed by confocal microscopy. Specific counterstaining of nucleus or cytoplasmic compartments was performed by using DRAQ5 fluorescence probe or anti-vimentin antibody, respectively. At least 300 cells were analyzed; a representative cell for HBZ staining is shown for each patient.

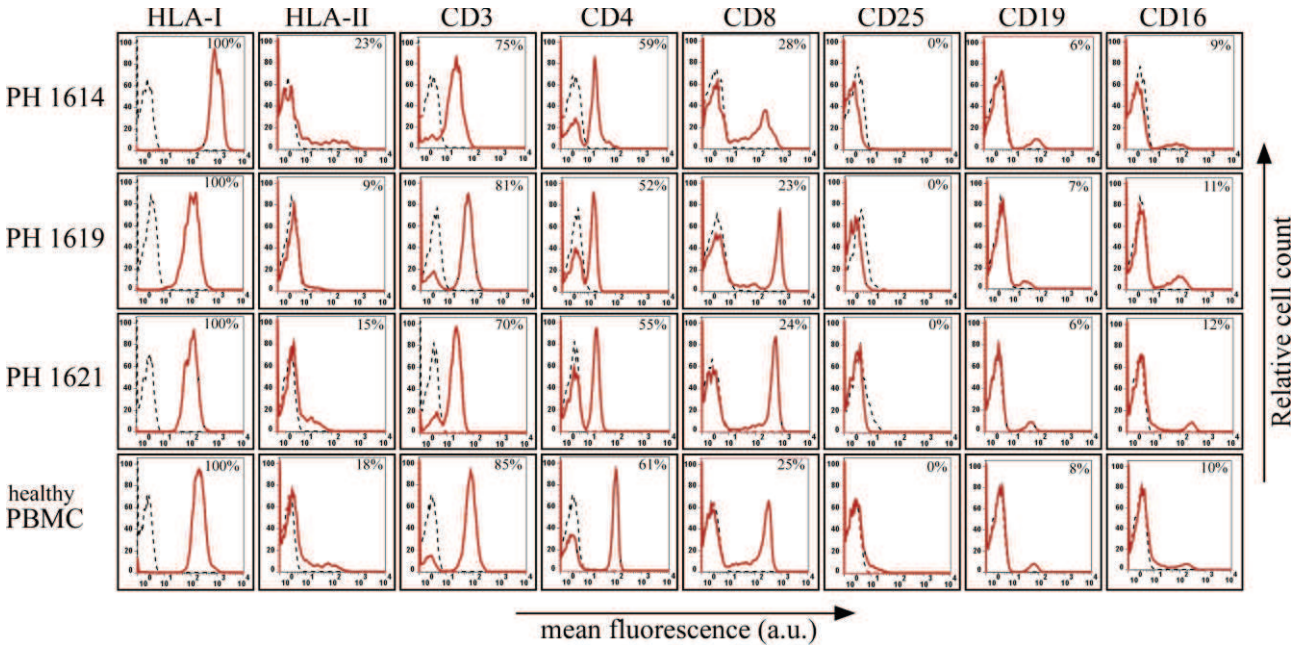

Figure 9. Expression of cells surface markers in PBMC of AC individuals and healthy control. The expression of HLA class I, HLA class II DR, CD3, CD4, CD8, CD25, CD19, and CD16 surface molecules on PBMC from AC patient PH1614, PH 1619 and PH 1621 and a healthy control was assessed by immunofluorescence and flow cytometry with antibodies specific for the various markers. Results are expressed as relative number of cells (ordinate) versus the mean intensity of fluorescence in arbitrary units (abscissa). In each histogram, negative controls, obtained by staining the cells with an appropriate isotype-matched antibody, are depicted as dashed line. The percentage of positive cells for the cell surface marker analyzed are indicated on the top right of every panel.

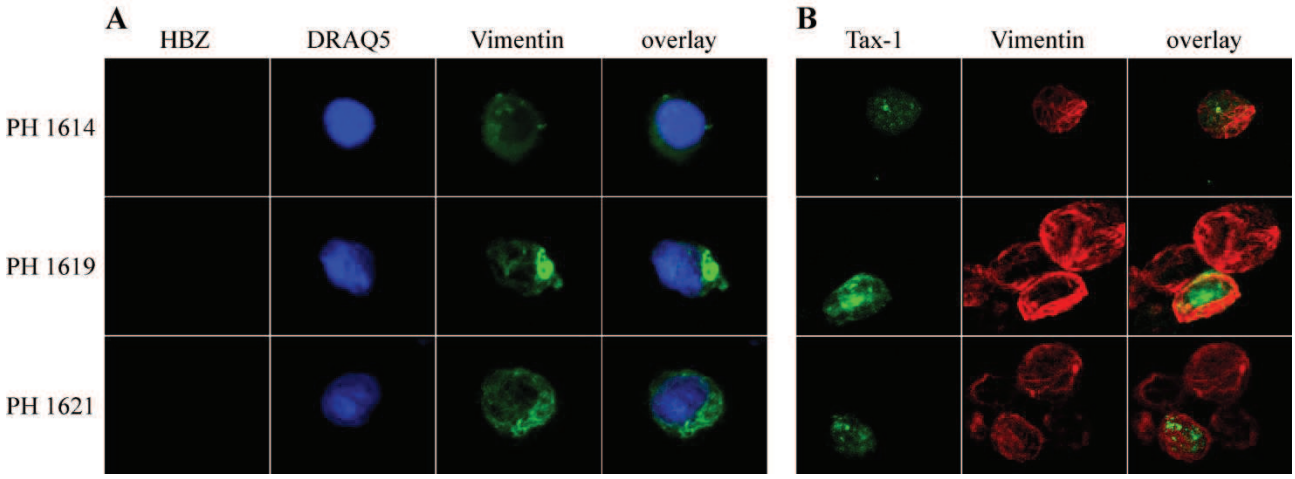

Figure 10. Lack of endogenous HBZ, but not of Tax-1, detection in PBMC of HTLV-1 positive asymptomatic carriers. (A) PBMC of three HTLV-1-positive asymptomatic carriers (PH1614, PH1619, and PH1621) were stained with the anti-HBZ 4D4-F3 and (B) the anti-Tax-1 A51-2 mAbs, followed by Alexa Fluor 546-conjugated goat anti-mouse IgG1antibody to detect HBZ protein (red), or by Alexa Fluor 488-conjugated goat-anti-mouse IgG2a to detect Tax-1 (green), and analyzed by confocal microscopy. Specific counterstaining of nucleus or cytoplasmic compartments was performed by using DRAQ5 fluorescence probe to detect the nucleus and anti-vimentin rabbit polyclonal antibody followed by goat anti-rabbit IgG conjugated to Alexa Fluor 488 (green, panel A) or to Alexa Fluor 546 (red, panel B) to stain the cytoplasmic compartment. At least 300 cells were analyzed; a representative cell is shown for each patient.

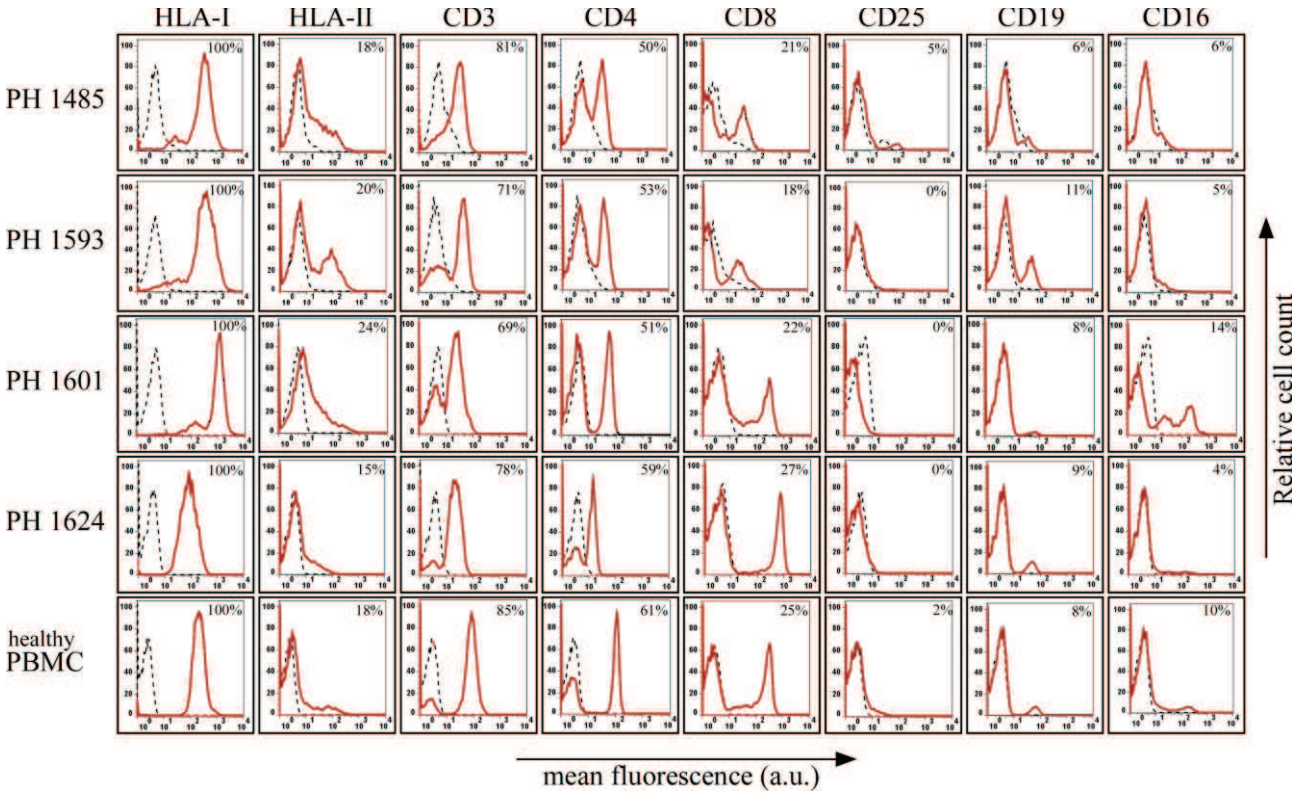

Figure 11. Expression of cells surface markers in PBMC of HAM/TSP patients and healthy control. The expression of HLA class I, HLA class II DR, CD3, CD4, CD8, CD25, CD19, and CD16 surface molecules on PBMC from AC 1485, 1593, 1601,1624 and a healthy control was assessed by immunofluorescence and flow cytometry with antibodies specific for the various markers. Results are expressed as relative number of cells (ordinate) versus the mean intensity of fluorescence in arbitrary units (abscissa). In each histogram, negative controls, obtained by staining the cells with an appropriate isotype-matched antibody, are depicted as dashed line. The percentage of positive cells for the cell surface marker analyzed are indicated on the top right of every panel.

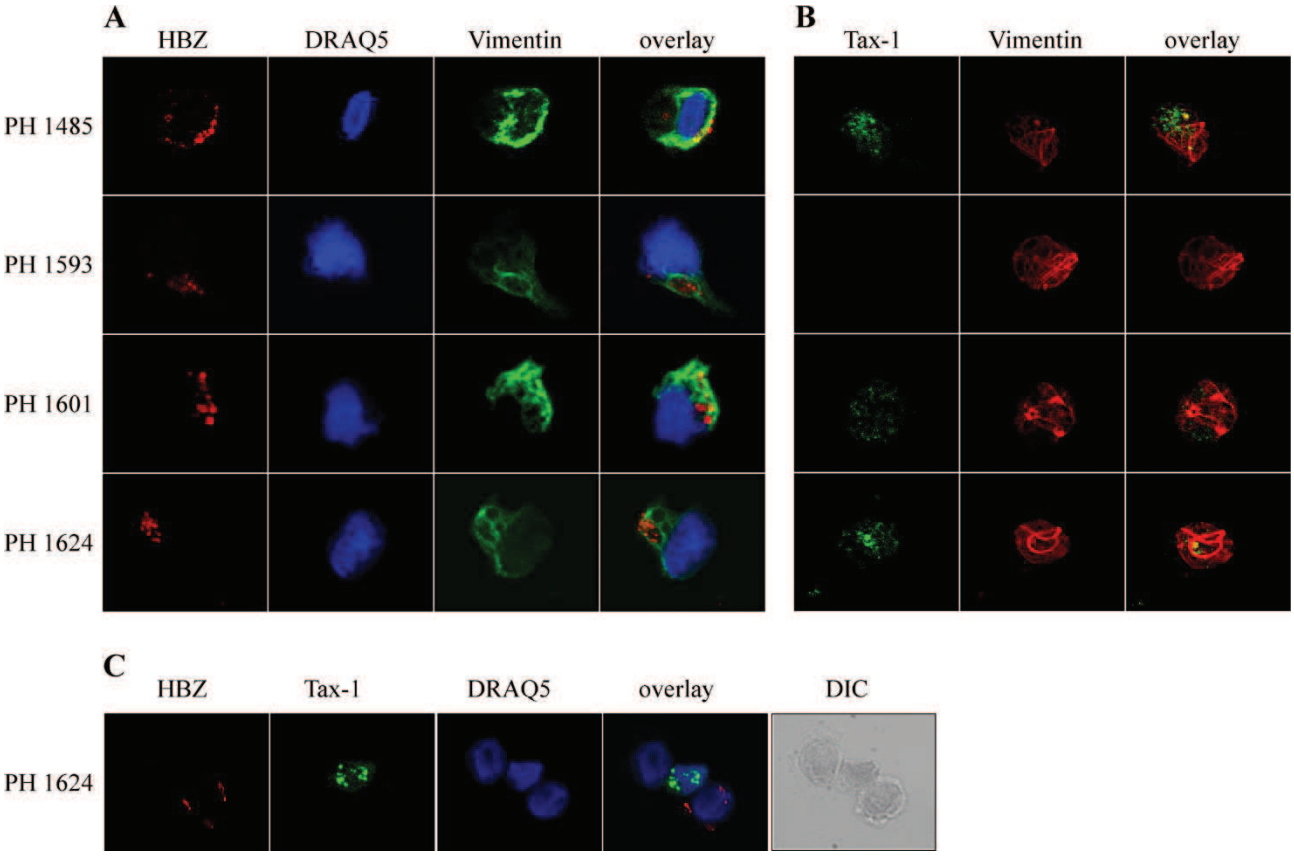

Figure 12. Subcellular localization of endogenous HBZ and Tax-1 in PBMC of HAM/TSP patients. (A) PBMC of four HAM/TSP patients (PH1485, PH1593, PH1601, and PH1624) were stained with the 4D4-F3 anti-HBZ mAb followed by Alexa Fluor 546-conjugated goat anti-mouse IgG1 antibody (red) and (B) with the A51-2 anti-Tax-1 mAb followed by Alexa Fluor 488-conjugated goat-anti-mouse IgG2a antibody (green), and analyzed by confocal microscopy. Specific counterstaining of nucleus or cytoplasmic compartments was performed by using DRAQ5 fluorescence probe to detect the nucleus and anti-vimentin rabbit polyclonal antibody followed by goat anti-rabbit IgG conjugated to Alexa Fluor 488 (green, panel A) or to Alexa Fluor 546 (red, panel B) to stain the cytoplasmic compartment. At least 300 cells were analyzed; a representative cell for HBZ or for Tax-1 staining is shown for each patient.(C) Low magnification field to show the co-existence of cells mutually exclusive for the expression of cytoplasmic HBZ and Tax-1 in PBMC of patient PH1624. Cells were co-stained with 4D4-F3 anti-HBZ mAb and with A51-2 anti-Tax-1 mAb followed by specific secondary antibodies staining as described in (A) and (B).

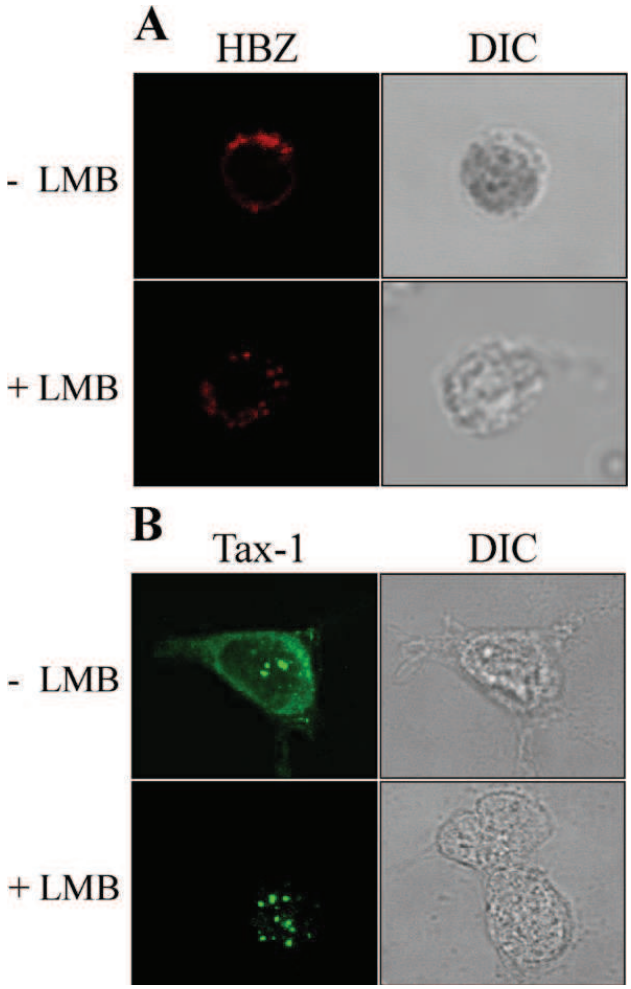

Figure 13. In HAM/TSP patient PBMC, HBZ is a resident cytoplasmic protein and does not shuttle to the nucleus throughout the exportin system. (A) PBMC of HAM/TSP patient PH1624 were either treated (+ LMB) or untreated (- LMB) with LMB, an inhibitor of nuclear export, before fixing and staining with the anti-HBZ 4D4-F3 mAb followed by Alexa Fluor 546-conjugated goat anti-mouse IgG1antibody (red). (B) As control of inhibition of nuclear export by LMB, 293T cells transfected with the plasmid coding for Tax-1 viral protein were treated with LMB (+LMB) or left untreated (-LMB). Cells were fixed and stained with A51-2 anti Tax-1 mAb followed by Alexa Fluor 488-conjugated goat-anti-mouse IgG2a (green), and analyzed by confocal microscopy. DIC represents the differential interference contrast image.

PH1624

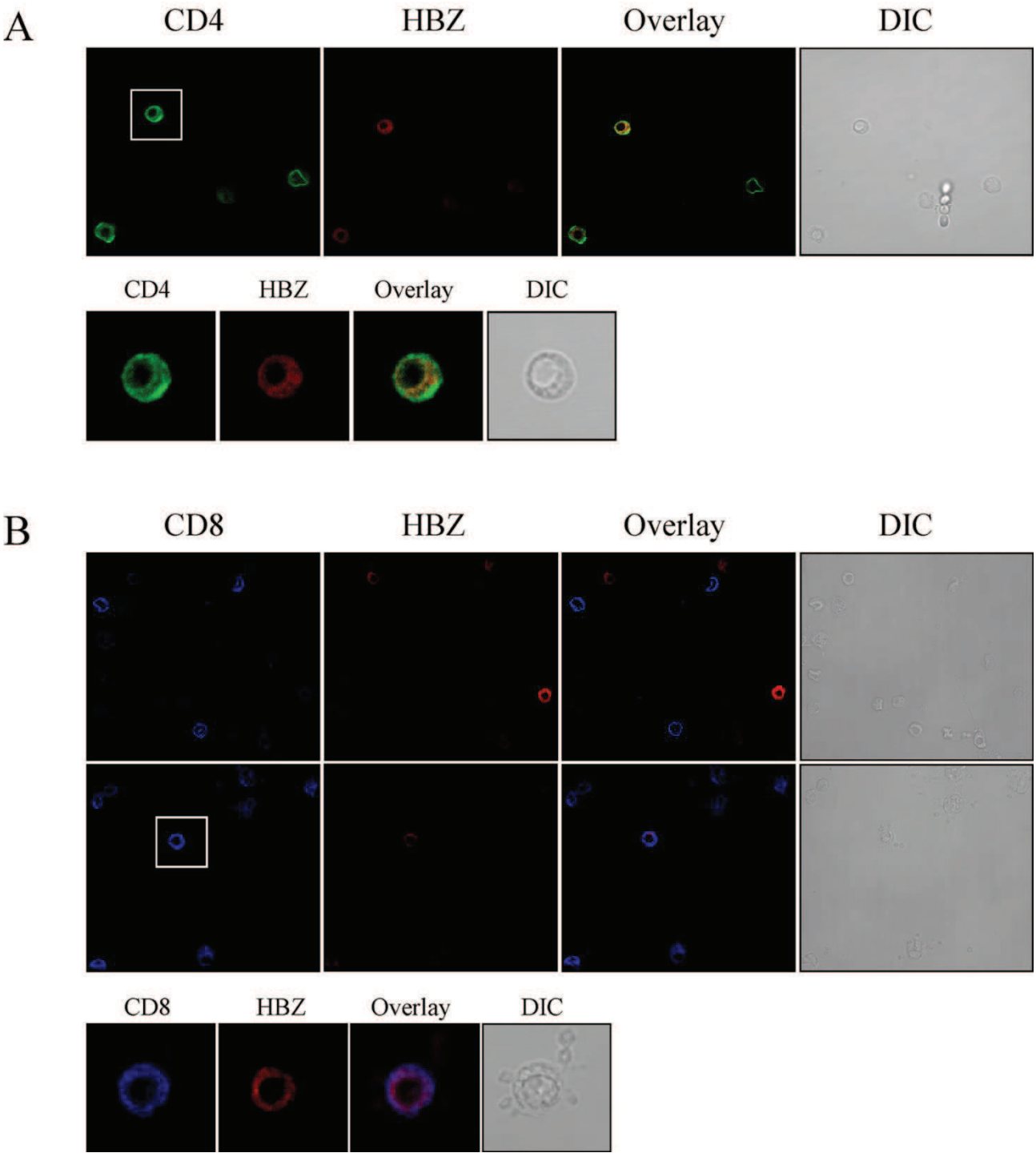
A
CD4
HBZ
Overlay
DIC
CD4
HBZ
Overlay
DIC
B
CD8
HBZ
Overlay
DIC
CD8
HBZ
Overlay
DIC

Figure 14. HBZ is preferentially expressed in CD4+ T cells of HAM/TSP patient PH1624. Confocal microscopy analysis of PBMC from HAM/TSP patient PH1624. (A) co-staining with the 4D4-F3 anti-HBZ mAb followed by Alexa Fluor 546-conjugated goat anti-mouse IgG1 antibody (red) and with the anti-CD4 mAb followed by Alexa Fluor 488-conjugated goat-anti-rabbit IgG antibody (green); upper panels, extended field; lower panels, enlarged field focused on the single cell depicted in the square of the left upper panel and positive for both CD4 and HBZ. (B) co-staining with the 4D4-F3 anti-HBZ mAb followed by Alexa Fluor 546-conjugated goat anti-mouse IgG1 antibody (red) and with the anti-CD8 rabbit monoclonal antibody directly conjugated to Alexa Fluor 647 (blue); upper panels depict extended fields with CD8+ cells negative for HBZ; middle panels, extended fields with many CD8+ cells negative for HBZ and the single CD8+/HBZ+ cell (square); lower panels, enlarged field on the single CD8+/HBZ+ cell.

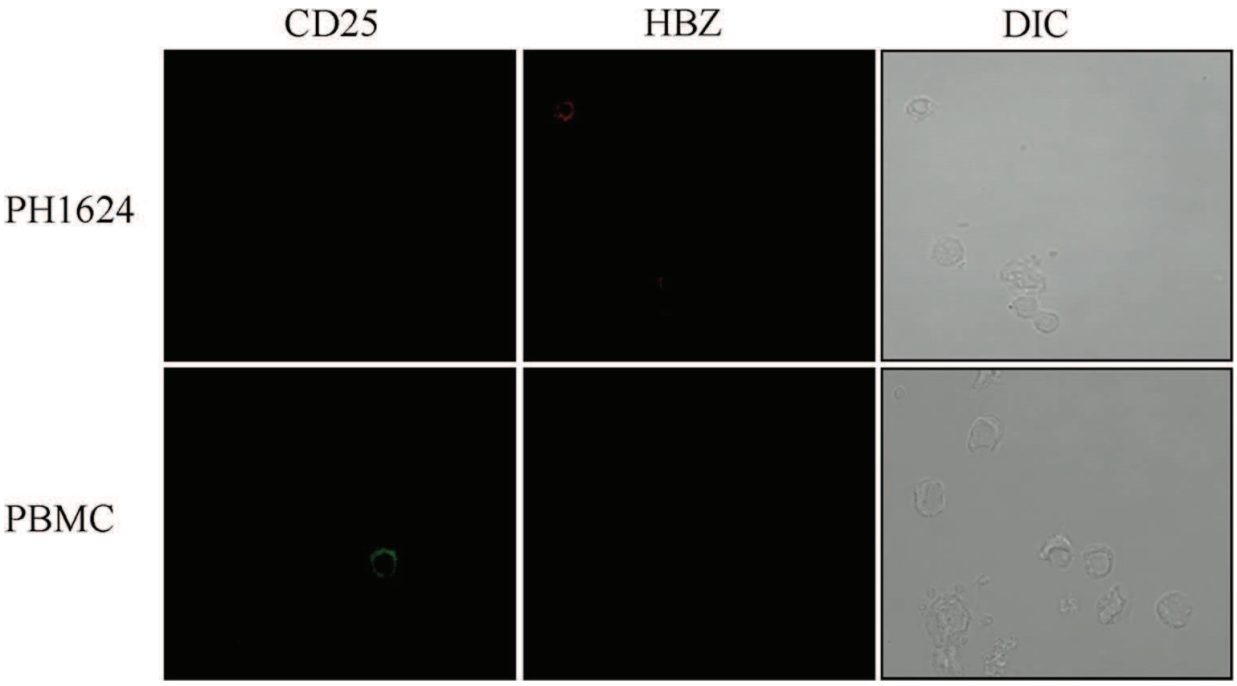

Figure 15. Lack of CD25+ cell in PBMC of patient PH1624, as assessed by confocal microscopy. PBMC of HAM/TSP patient PH1624 and of healthy control were co-stained with the anti-HBZ 4D4-F3 mAb followed by Alexa Fluor 546-conjugated goat anti-mouse IgG1 antibody (red) and with the anti-CD25 monoclonal antibody directly conjugated to Alexa Fluor 488 (green) and analyzed by confocal microscopy. Upper left panel shows the negativity of CD25 staining in PH1624 patient as compared with a positive cell for the same marker in PBMC of healthy control (PBMC, lower left panel).

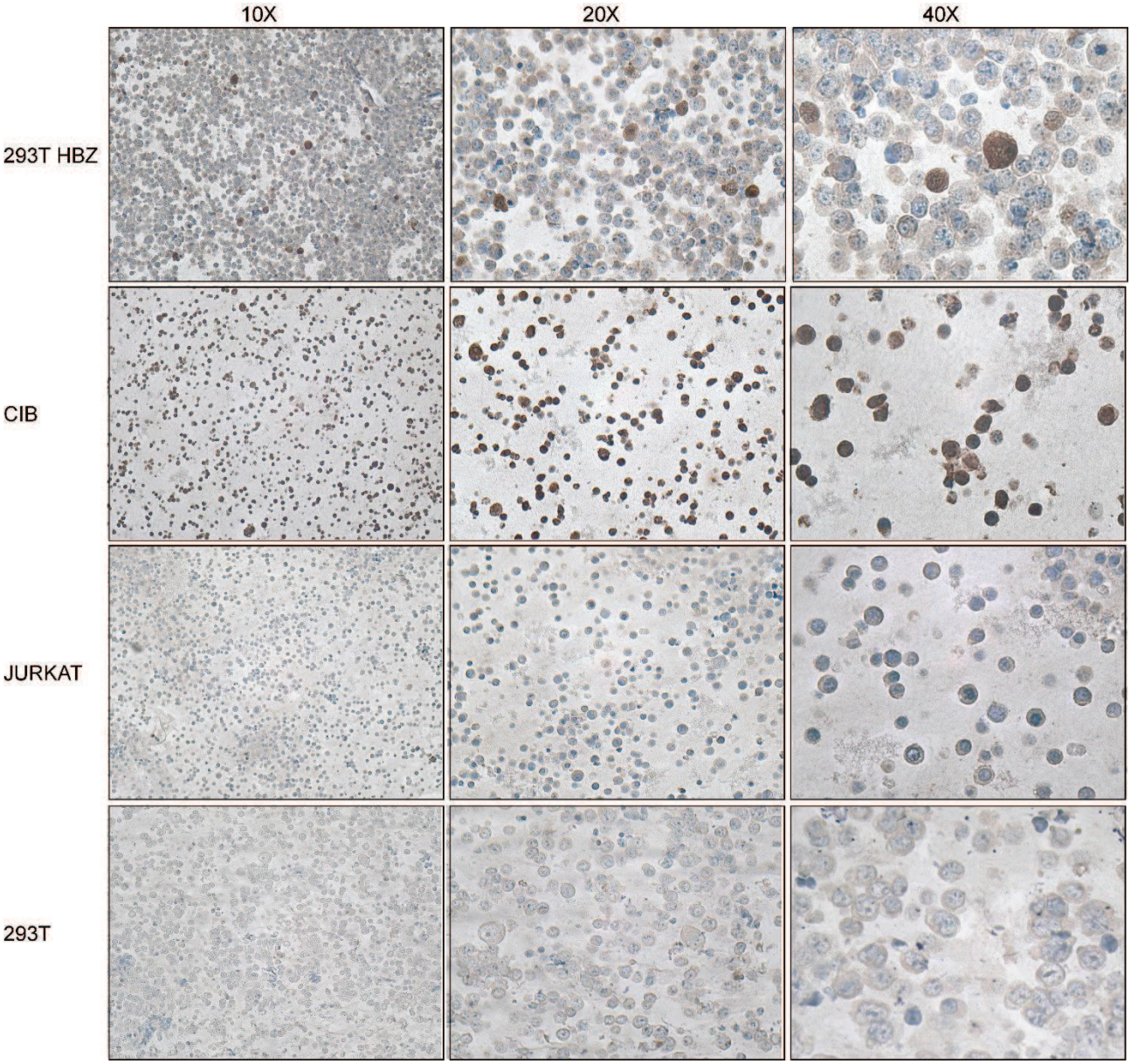

Figure 16. Immunohistochemical (IHC) staining of HBZ ectopically expressed in 293T and endogenously expressed in CIB cells. 293T. Cells were stained with 4D4-F3 anti-HBZ mAb. All CIB cells show positivity for HBZ (brown staining). Non-transfected 293T and Jurkat T cells were used as negative control while HBZ transfected 293T cells were used as positive control of HBZ expression (cells with brown staining).

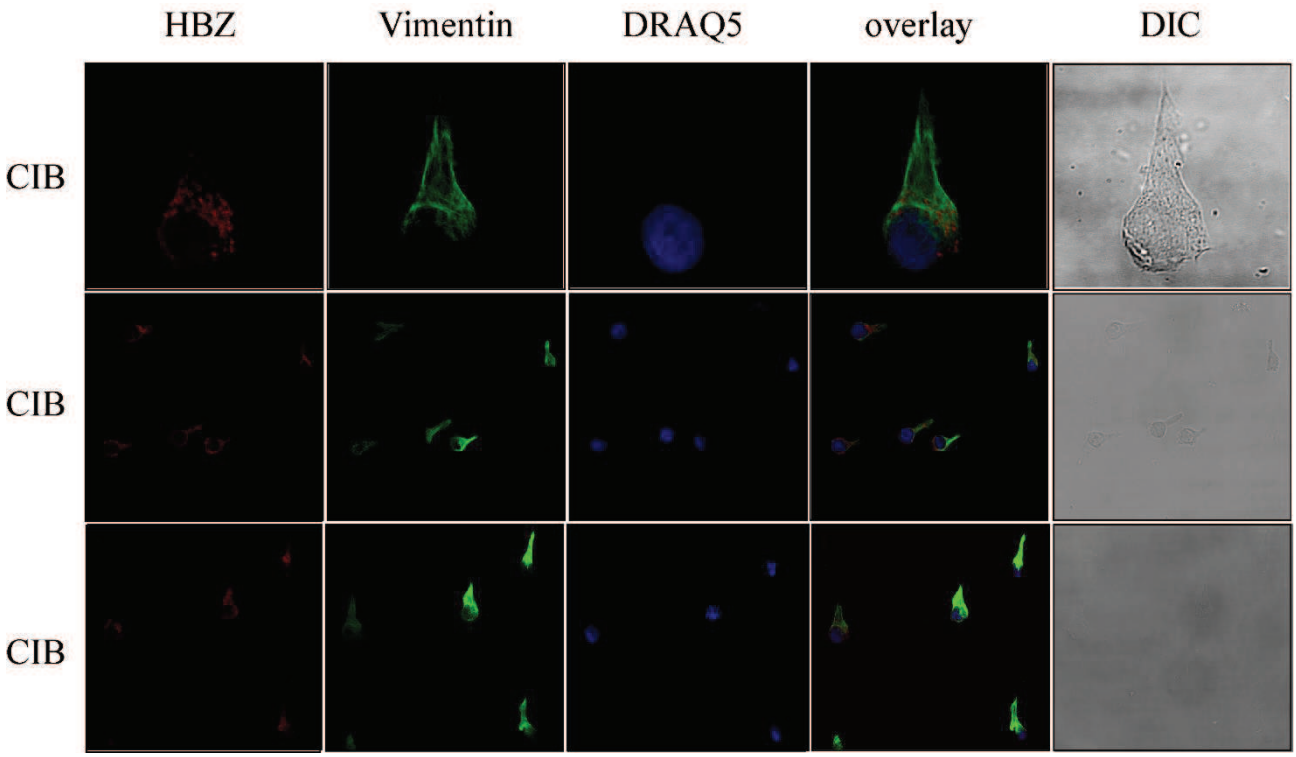

Figure 17. Cytoplasmic localization of endogenous HBZ in CIB cells. CIB cells were stained with the 4D4-F3 anti-HBZ mAb followed by Alexa Fluor 546-conjugated goat anti-mouse IgG1 antibody (red). Specific counterstaining of nucleus or cytoplasmic compartments was performed by using DRAQ5 fluorescence probe to detect the nucleus and anti-vimentin rabbit polyclonal antibody followed by goat anti-rabbit IgG conjugated to Alexa Fluor 488 to stain the cytoplasmic compartment. At least 1000 cells were analyzed.

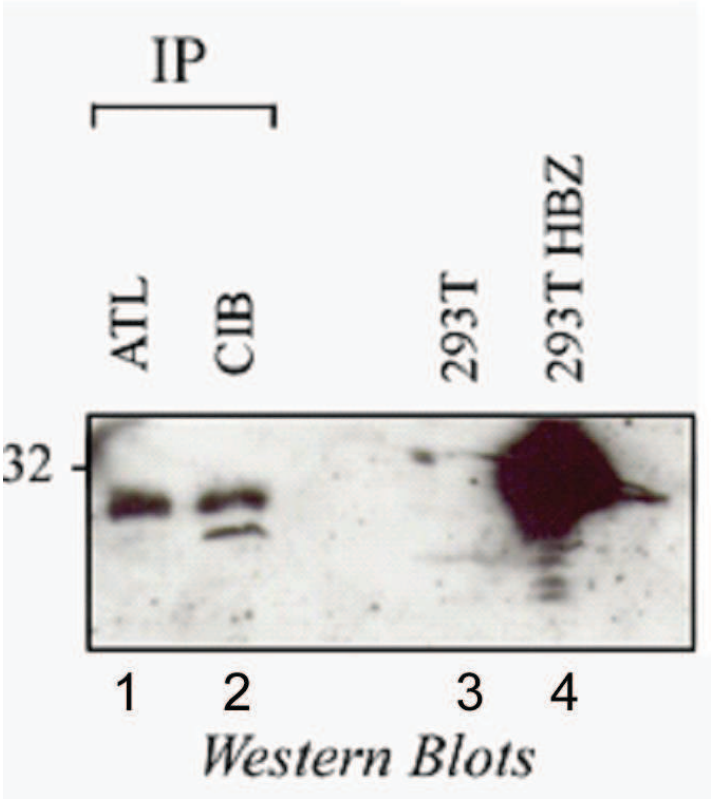

Figure 18. HBZ is expressed in ATL and CIB cells line in a similar amount. Cell extracts from ATL (line 1) and CIB (Line 2) cells were immunoprecipitated (IP) with anti-HBZ monoclonal antibody and the immunocomplex were analyzed by western blotting with anti-HBZ monoclonal antibody. Cell lysates of 293T cells expressing (293T HBZ) (line 4) or not (293T) (line 3) HBZ were analysed by western blotting with anti-HBZ monoclonal antibodies.

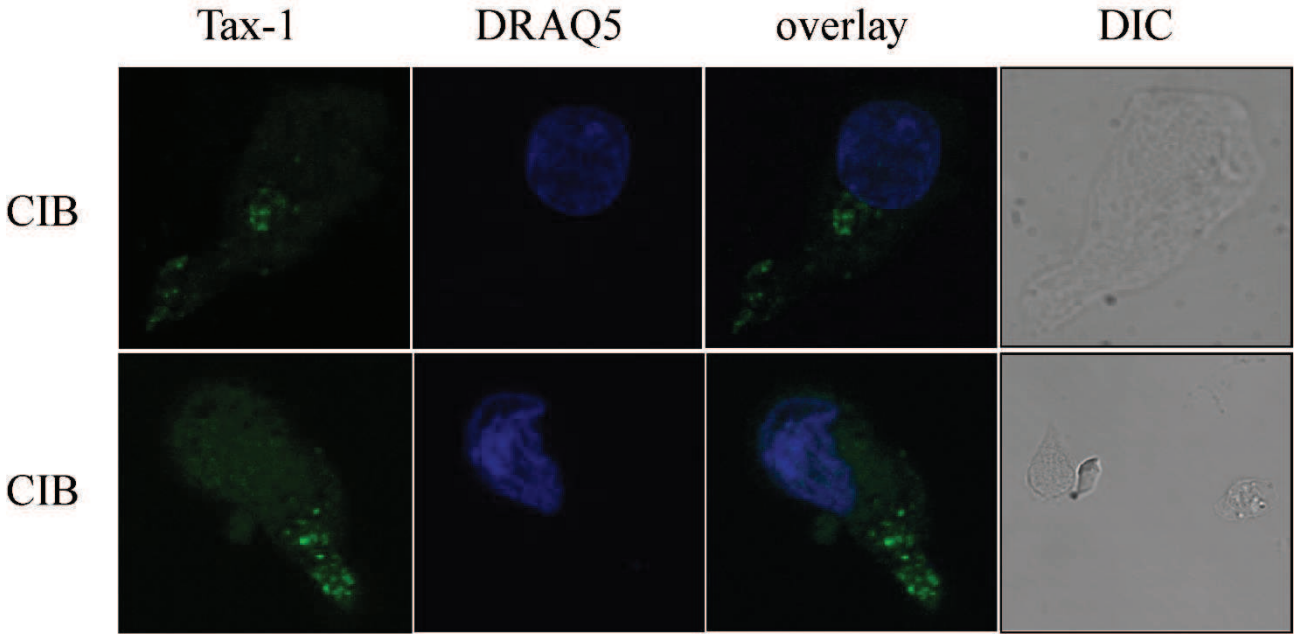

Figure 19. Subcellular localization of endogenous Tax-1 in CIB cells. CIB cells were stained with the A51-2 anti-Tax-1 mAb followed by Alexa Fluor 488-conjugated goat-anti-mouse IgG2a antibody (green), and analyzed by confocal microscopy. Specific counterstaining of nucleus or cytoplasmic compartments was performed by using DRAQ5 fluorescence probe to detect the nucleus. Two representive cells are shown. At least 100 cells were analyzed.

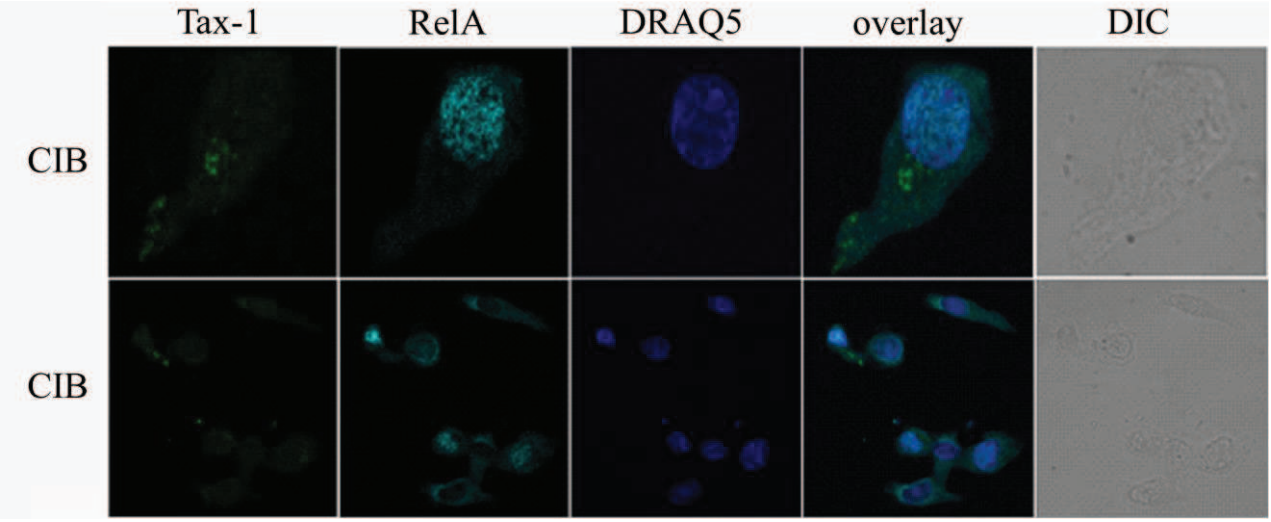

Figure 20. Tax-1 expression in CIB cells can induce RelA migration in the nucleus of CIB cells. Cells were co-stained with anti p65 mAb followed by Alexa Fluor 546-conjugated goat anti-rabbit IgG antibody (light blue) and with A51-2 anti-Tax-1 mAb followed by Alexa Fluor 488-conjugated goat-anti-mouse IgG2a antibody (green) and analyzed by confocal microscopy. Two representative fields are shown. The upper series of panels focuses on a single cell. The bottom series of panels shows seven cells.

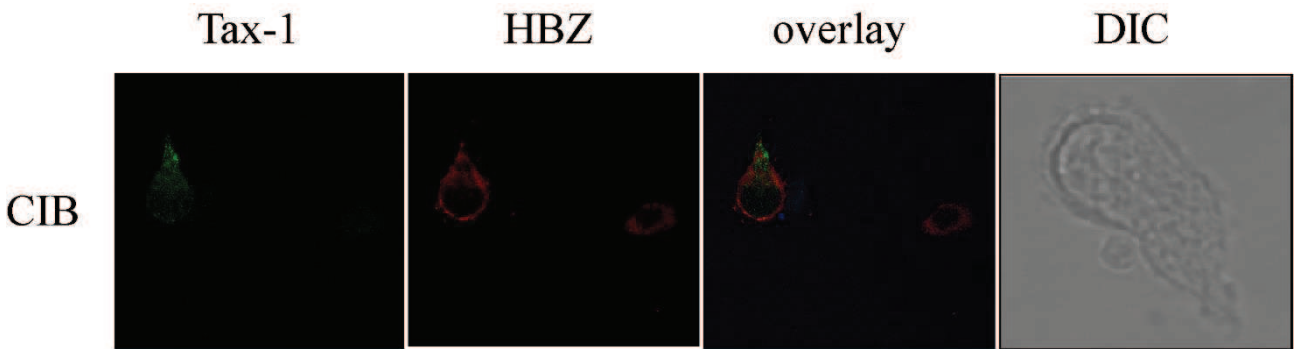

Figure 21. Co-expression of endogenous HBZ and Tax-1 in CIB cells in distinct cytoplasmic compartments. Representative image of HBZ and Tax-1 co-expression in CIB cells. Cells were co-stained with 4D4-F3 anti-HBZ mAb followed by Alexa Fluor 546-conjugated goat anti-mouse IgG1 antibody (red) and with A51-2 anti-Tax-1 mAb followed by Alexa Fluor 488-conjugated goat-anti-mouse IgG2a antibody (green) and analyzed by confocal microscopy. A representative cell is shown.

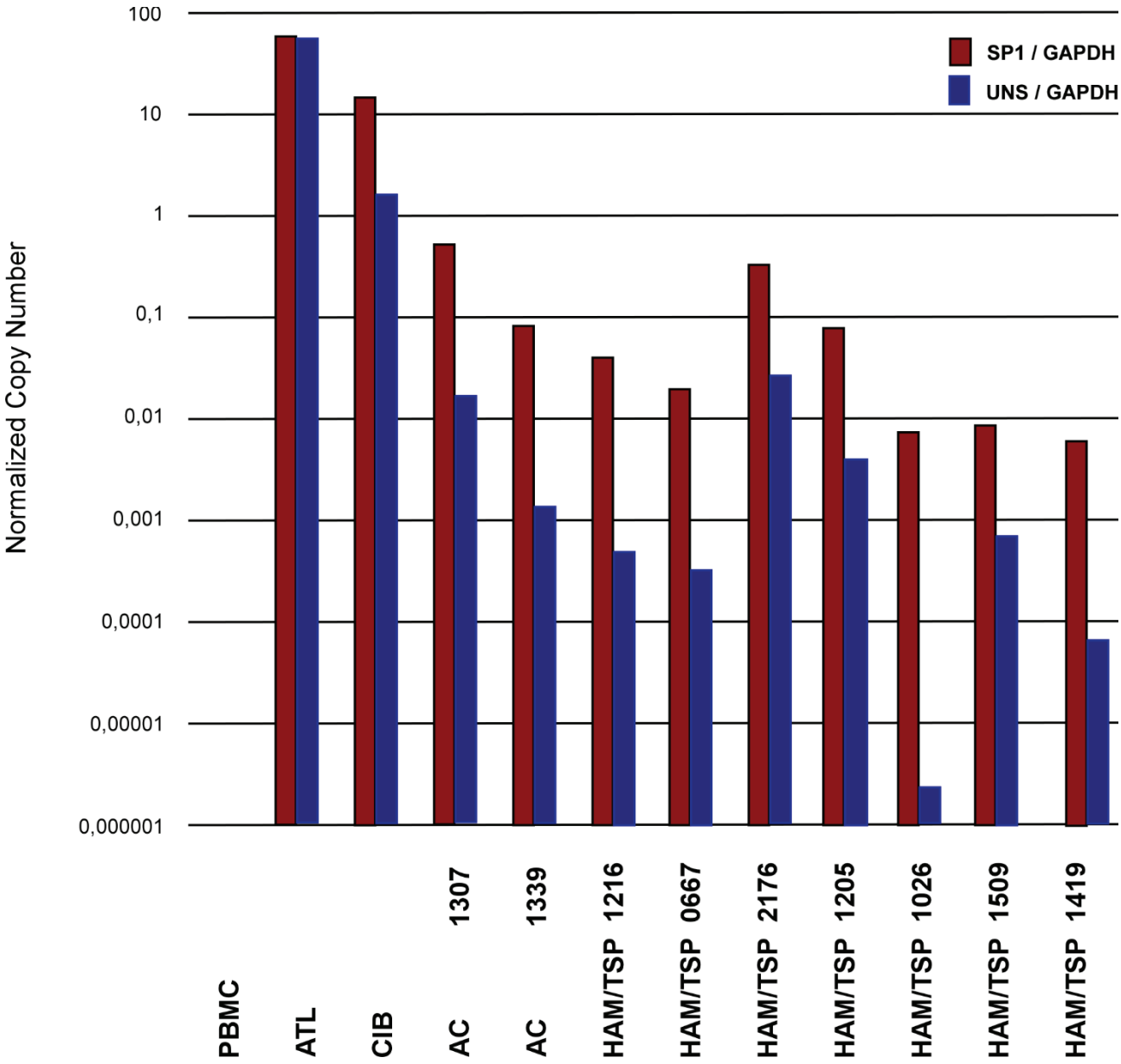

Figure 22. mRNA expression levels of Unspliced and Spliced-1 HBZ in ATL and CIB cell lines and in AC and HAM/TSP patients. mRNA levels of both unspliced and spliced HBD isoforms were analyzed in PBMC isolated from ATL, AC and HAM/TSP patients by QRT-PCR. Bar graphs show normalized copy numbers of the different mRNAs analyzed, as indicated in Materials and Methods.

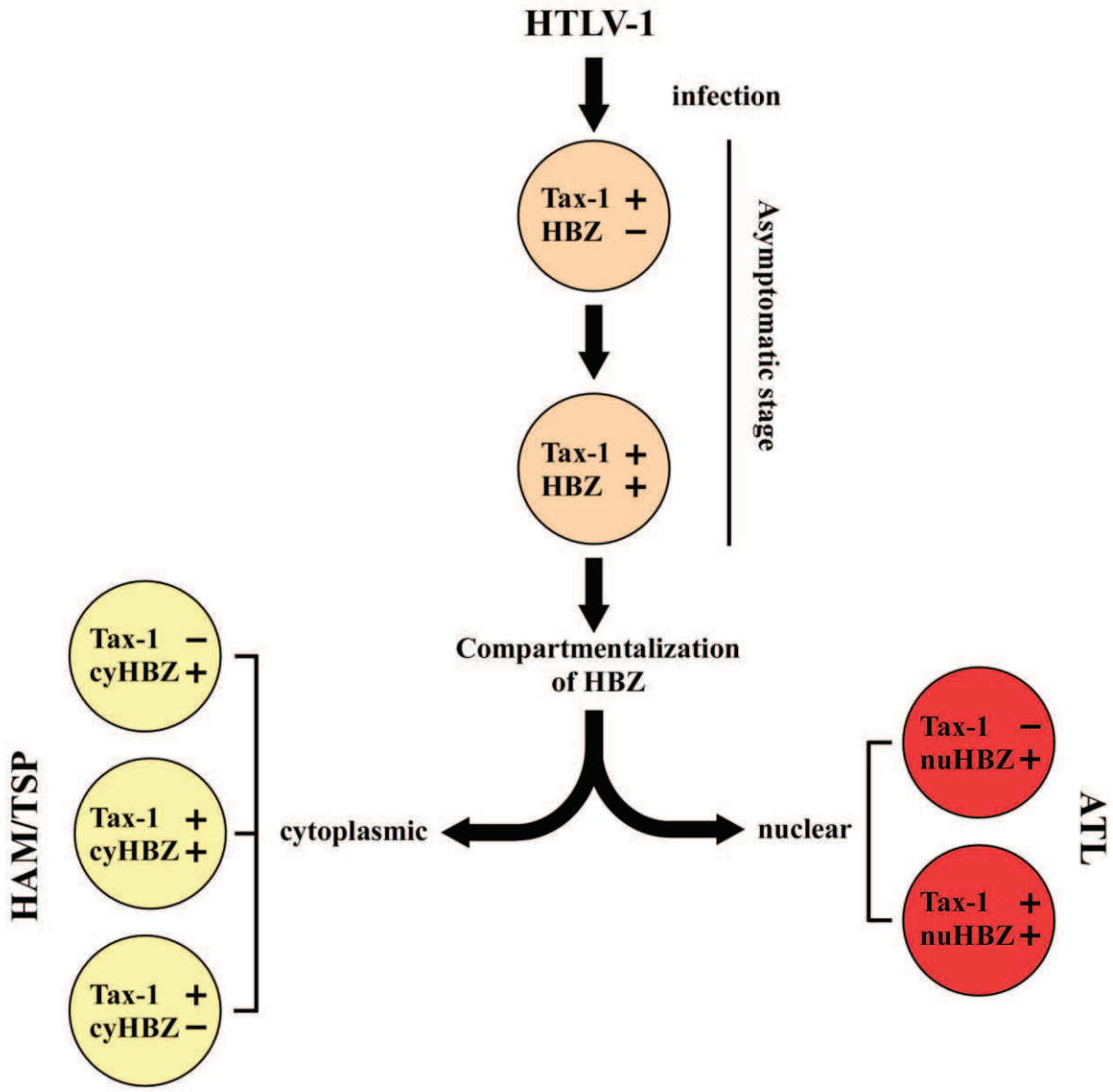

Figure 23. A hypothetical model of disease progression in HTLV-1 infected people. The model is based on the expression and localization of Tax-1 and HBZ proteins at the single cell level. Primary HTLV-1 infection is associated to the expression of Tax-1. The progression of the disease leads to a different stage characterized by the concomitant expression of Tax-1 and HBZ. The subsequent localization of HBZ in the nucleus (nuHBZ) or the cytoplasm (cyHBZ) differentiates the disease versus the leukemic or the inflammatory state.

Patient	Ab titer*	Pathology	HBZ+ cells (%)			Tax-1+ cells (%)		
			Total	Nucleus	Cyto	Total	Nucleus	Cyto
PH1485	640	HAM/TSP	11	0	11	14	14	5^
PH1593	2560	HAM/TSP	4	0	4	0	-	-
PH1601	2560	HAM/TSP	0,4	0	0,4	1	1	0
PH1624	2560	HAM/TSP	9	0	9	20	20	12^
PH1393	320	ATL	83	83	0	0	-	-
PH1505	1280	ATL	80	83	0	0	-	-
PH1614	640	AC	0	-	-	11	11	5^
PH1619	640	AC	0	-	-	1	1	0
PH1621	1024	AC	0	-	-	6	6	2^

* reverse dilution values of anti-HTLV-1 antibody defined as described in Materials and Methods.

^ percent of cells with Tax-1 localization in cytoplasm and nucleus. Tax-1 was never localized in cytoplasm alone

Table 1. Percent and subcellular distribution of HBZ+ and Tax-1+ PBMC in HTLV-1 associated pathologies.

6 ACKNOWLEDGEMENT

This project would not have been possible without the kind support and help of many people that helped me throughout. I would like to extend my sincere thanks to all of them.

I am highly great full to Dr. Greta Forlani for her guidance and constant supervision as well as for providing information regarding the experiments and also for her support in completing the project.

My thanks and appreciations also go to my colleague Dr. Alessandra Tedeschi, Dr. Elise Ramia, Dr.Goutham U. Raval and Dr. Farah Bou Nasseredine who have willingly helped me with their abilities.

I would like to express my gratitude towards Professor Vincenzo Ciminale, Professor Donna D' Agostino and Dr. Ilaria Cavallari and Dr. Vittoria Raimondi from the Instituto Oncologico Veneto for their kind co-operation and supervision regarding the HBZ mRNA analysis.

Thanks also to Dr. Annamaria Chiaravalli and Dr. Giovanna Finzi from the Anatomopathology department in Varese for their co-operation and ability in Electron Microscopy and Immunohistochemistry.

Special Thanks to Dr. Giovanna Tosi, for the great energy she has, in science and in life.

I would like to express my special gratitude and thanks to Professor Roberto Accolla for giving me attention, time, endless patients and extremely helpful advice and knowledge.

7 REFERENCES

Araya, N., Sato, T., Yagishita, N., Ando, H., Utsunomiya, A., Jacobson, S., Yamano, Y., 2011. Human T-lymphotropic virus type 1 (HTLV-1) and regulatory T cells in HTLV-1-associated neuroinflammatory disease. Viruses 3, 1532-1548.

Baratella, M., Forlani, G., Raval, G.U., Tedeschi, A., Gout, O., Gessain, A., Tosi, G., Accolla, R.S., 2017. Cytoplasmic Localization of HTLV-1 HBZ Protein: A Biomarker of HTLV-1-Associated Myelopathy/Tropical Spastic Paraparesis (HAM/TSP). PLoS Negl Trop Dis 11, e0005285.

Barbeau, B., Peloponese, J.M., Mesnard, J.M., 2013. Functional comparison of antisense proteins of HTLV-1 and HTLV-2 in viral pathogenesis. Frontiers in microbiology 4, 226.

Basbous, J., Arpin, C., Gaudray, G., Piechaczyk, M., Devaux, C., Mesnard, J.M., 2003. The HBZ factor of human T-cell leukemia virus type I dimerizes with transcription factors JunB and c-Jun and modulates their transcriptional activity. The Journal of biological chemistry 278, 43620-43627.

Clerc, I., Polakowski, N., Andre-Arpin, C., Cook, P., Barbeau, B., Mesnard, J.M., Lemasson, I., 2008. An interaction between the human T cell leukemia virus type 1 basic leucine zipper factor (HBZ) and the KIX domain of p300/CBP contributes to the down-regulation of tax-dependent viral transcription by HBZ. The Journal of biological chemistry 283, 23903-23913.

Cooper, S.A., van der Loeff, M.S., Taylor, G.P., 2009. The neurology of HTLV-1 infection. Practical neurology 9, 16-26.

Forlani, G., Abdallah, R., Accolla, R.S., Tosi, G., 2016. The Major Histocompatibility Complex Class II Transactivator CIITA Inhibits the Persistent Activation of NF-kappaB by the Human T Cell Lymphotropic Virus Type 1 Tax-1 Oncoprotein. J Virol 90, 3708-3721.

Franchini, G., Fukumoto, R., Fullen, J.R., 2003. T-cell control by human T-cell leukemia/lymphoma virus type 1. International journal of hematology 78, 280-296.

Gaudray, G., Gachon, F., Basbous, J., Biard-Piechaczyk, M., Devaux, C., Mesnard, J.M., 2002. The Complementary Strand of the Human T-Cell Leukemia Virus Type 1 RNA Genome Encodes a bZIP Transcription Factor That Down-Regulates Viral Transcription. Journal of Virology 76, 12813-12822.

Gazon, H., Lemasson, I., Polakowski, N., Cesaire, R., Matsuoka, M., Barbeau, B., Mesnard, J.M., Peloponese, J.M., Jr., 2012. Human T-cell leukemia virus type 1 (HTLV-1) bZIP factor requires cellular transcription factor JunD to upregulate HTLV-1 antisense transcription from the 3' long terminal repeat. J Virol 86, 9070-9078.

Gessain, A., Cassar, O., 2012. Epidemiological Aspects and World Distribution of HTLV-1 Infection. Front Microbiol 3, 388.

Giam, C.Z., Semmes, O.J., 2016. HTLV-1 Infection and Adult T-Cell Leukemia/Lymphoma-A Tale of Two Proteins: Tax and HBZ. Viruses 8.

Goncalves, D.U., Proietti, F.A., Ribas, J.G., Araujo, M.G., Pinheiro, S.R., Guedes, A.C., Carneiro-Proietti, A.B., 2010. Epidemiology, treatment, and prevention of human T-cell leukemia virus type 1-associated diseases. Clinical microbiology reviews 23, 577-589.

Hagiya, K., Yasunaga, J., Satou, Y., Ohshima, K., Matsuoka, M., 2011. ATF3, an HTLV-1 bZip factor binding protein, promotes proliferation of adult T-cell leukemia cells. Retrovirology 8, 19.

Hilburn, S., Rowan, A., Demontis, M.A., MacNamara, A., Asquith, B., Bangham, C.R., Taylor, G.P., 2011. In vivo expression of human T-lymphotropic virus type 1 basic leucine-zipper protein generates specific CD8+ and CD4+ T-lymphocyte responses that correlate with clinical outcome. The Journal of infectious diseases 203, 529-536.

Kannian, P., Green, P.L., 2010. Human T Lymphotropic Virus Type 1 (HTLV-1): Molecular Biology and Oncogenesis. Viruses 2, 2037-2077.

Karube, K., Ohshima, K., Tsuchiya, T., Yamaguchi, T., Kawano, R., Suzumiya, J., Utsunomiya, A., Harada, M., Kikuchi, M., 2004. Expression of FoxP3, a key molecule in CD4CD25 regulatory T cells, in adult T-cell leukaemia/lymphoma cells. British journal of haematology 126, 81-84.

Kuhlmann, A.S., Villaudy, J., Gazzolo, L., Castellazzi, M., Mesnard, J.M., Duc Dodon, M., 2007. HTLV-1 HBZ cooperates with JunD to enhance transcription of the human telomerase reverse transcriptase gene (hTERT). Retrovirology 4, 92.

Ma, G., Yasunaga, J., Fan, J., Yanagawa, S., Matsuoka, M., 2013. HTLV-1 bZIP factor dysregulates the Wnt pathways to support proliferation and migration of adult T-cell leukemia cells. Oncogene 32, 4222-4230.

Ma, G., Yasunaga, J., Matsuoka, M., 2016. Multifaceted functions and roles of HBZ in HTLV-1 pathogenesis. Retrovirology 13, 16.

Macnamara, A., Rowan, A., Hilburn, S., Kadolsky, U., Fujiwara, H., Suemori, K., Yasukawa, M., Taylor, G., Bangham, C.R., Asquith, B., 2010. HLA class I binding of HBZ determines outcome in HTLV-1 infection. PLoS pathogens 6, e1001117.

Mahieux, R., Gessain, A., 2009. The human HTLV-3 and HTLV-4 retroviruses: new members of the HTLV family. Pathologie-biologie 57, 161-166.

Matsuoka, M., Jeang, K.T., 2007. Human T-cell leukaemia virus type 1 (HTLV-1) infectivity and cellular transformation. Nature reviews. Cancer 7, 270-280.

Matsuoka, M., Yasunaga, J., 2013. Human T-cell leukemia virus type 1: replication, proliferation and propagation by Tax and HTLV-1 bZIP factor. Current opinion in virology 3, 684-691.

Mota-Miranda, A.C., Barreto, F.K., Baptista, E., Farre-Vale, L., Monteiro-Cunha, J.P., Galvao-Castro, B., Alcantara, L.C., 2013. Molecular study of HBZ and gp21 human T cell leukemia virus type 1 proteins isolated from different clinical profile infected individuals. AIDS Res Hum Retroviruses 29, 1370-1372.

Murata, K., Hayashibara, T., Sugahara, K., Uemura, A., Yamaguchi, T., Harasawa, H., Hasegawa, H., Tsuruda, K., Okazaki, T., Koji, T., Miyanishi, T., Yamada, Y., Kamihira, S., 2006. A novel alternative splicing isoform of human T-cell leukemia virus type 1 bZIP factor (HBZ-SI) targets distinct subnuclear localization. J Virol 80, 2495-2505.

Nicolas, D., Ambrosioni, J., Paredes, R., Marcos, M.A., Manzardo, C., Moreno, A., Miro, J.M., 2015. Infection with human retroviruses other than HIV-1: HIV-2, HTLV-

1, HTLV-2, HTLV-3 and HTLV-4. Expert review of anti-infective therapy 13, 947-963.

Ozden, S., Cochet, M., Mikol, J., Teixeira, A., Gessain, A., Pique, C., 2004. Direct evidence for a chronic CD8+-T-cell-mediated immune reaction to tax within the muscle of a human T-cell leukemia/lymphoma virus type 1-infected patient with sporadic inclusion body myositis. J Virol 78, 10320-10327.

Pinheiro, S.R., Martins-Filho, O.A., Ribas, J.G., Catalan-Soares, B.C., Proietti, F.A., Namen-Lopes, S., Brito-Melo, G.E., Carneiro-Proietti, A.B., Giph, 2006. Immunologic markers, uveitis, and keratoconjunctivitis sicca associated with human T-cell lymphotropic virus type 1. American journal of ophthalmology 142, 811-815.

Poiesz, B.J., Ruscetti, F.W., Gazdar, A.F., Bunn, P.A., Minna, J.D., Gallo, R.C., 1980. Detection and isolation of type C retrovirus particles from fresh and cultured lymphocytes of a patient with cutaneous T-cell lymphoma. Proc Natl Acad Sci U S A 77, 7415-7419.

Proietti, F.A., Carneiro-Proietti, A.B., Catalan-Soares, B.C., Murphy, E.L., 2005. Global epidemiology of HTLV-I infection and associated diseases. Oncogene 24, 6058-6068.

Raval, G.U., Bidoia, C., Forlani, G., Tosi, G., Gessain, A., Accolla, R.S., 2015. Localization, quantification and interaction with host factors of endogenous HTLV-1 HBZ protein in infected cells and ATL. Retrovirology 12, 59.

Satou, Y., Yasunaga, J., Yoshida, M., Matsuoka, M., 2006. HTLV-I basic leucine zipper factor gene mRNA supports proliferation of adult T cell leukemia cells.

Proceedings of the National Academy of Sciences of the United States of America 103, 720-725.

Satou, Y., Yasunaga, J., Zhao, T., Yoshida, M., Miyazato, P., Takai, K., Shimizu, K., Ohshima, K., Green, P.L., Ohkura, N., Yamaguchi, T., Ono, M., Sakaguchi, S., Matsuoka, M., 2011. HTLV-1 bZIP factor induces T-cell lymphoma and systemic inflammation in vivo. PLoS pathogens 7, e1001274.

Sugata, K., Satou, Y., Yasunaga, J., Hara, H., Ohshima, K., Utsunomiya, A., Mitsuyama, M., Matsuoka, M., 2012. HTLV-1 bZIP factor impairs cell-mediated immunity by suppressing production of Th1 cytokines. Blood 119, 434-444.

Takeda, S., Maeda, M., Morikawa, S., Taniguchi, Y., Yasunaga, J., Nosaka, K., Tanaka, Y., Matsuoka, M., 2004. Genetic and epigenetic inactivation of tax gene in adult T-cell leukemia cells. International journal of cancer 109, 559-567.

Tanaka, A., Takahashi, C., Yamaoka, S., Nosaka, T., Maki, M., Hatanaka, M., 1990. Oncogenic transformation by the tax gene of human T-cell leukemia virus type I in vitro. Proceedings of the National Academy of Sciences of the United States of America 87, 1071-1075.

Tosi, G., Forlani, G., Andresen, V., Turci, M., Bertazzoni, U., Franchini, G., Poli, G., Accolla, R.S., 2011. Major histocompatibility complex class II transactivator CIITA is a viral restriction factor that targets human T-cell lymphotropic virus type 1 Tax-1 function and inhibits viral replication. J Virol 85, 10719-10729.

Toulza, F., Nosaka, K., Takiguchi, M., Pagliuca, T., Mitsuya, H., Tanaka, Y., Taylor, G.P., Bangham, C.R., 2009. FoxP3+ regulatory T cells are distinct from leukemia cells

in HTLV-1-associated adult T-cell leukemia. International journal of cancer 125, 2375-2382.

Yamano, Y., Araya, N., Sato, T., Utsunomiya, A., Azakami, K., Hasegawa, D., Izumi, T., Fujita, H., Aratani, S., Yagishita, N., Fujii, R., Nishioka, K., Jacobson, S., Nakajima, T., 2009. Abnormally high levels of virus-infected IFN-gamma+ CCR4+ CD4+ CD25+ T cells in a retrovirus-associated neuroinflammatory disorder. PloS one 4, e6517.

Yasunaga, J., Matsuoka, M., 2011. Molecular mechanisms of HTLV-1 infection and pathogenesis. International journal of hematology 94, 435-442.

Zhang, L.-l., Wei, J.-y., Wang, L., Huang, S.-l., Chen, J.-l., 2017. Human T-cell lymphotropic virus type 1 and its oncogenesis. Acta Pharmacologica Sinica 38, 1093-1103.

Zhao, T., Satou, Y., Sugata, K., Miyazato, P., Green, P.L., Imamura, T., Matsuoka, M., 2011. HTLV-1 bZIP factor enhances TGF-beta signaling through p300 coactivator. Blood 118, 1865-1876.